Diploma thesis

Calcium homeostasis in autophagy-deficient mouse cardiomyocytes

submitted by

Simon C. Kraler

for the academic degree of

Doctor medicinae universae

(Dr. med. univ.)

at the

Medical University of Graz

Conducted at the

Division of Cardiology

Department of Internal Medicine

under the supervision of

Assoc. Prof. Dr. Simon Sedej

Senka Ljubojević-Holzer, PhD

August 27, 2019

I hereby declare that this thesis is my own original work and that I have fully acknowledged by name all of those individuals and organisations that have contributed to the research for this thesis. Due acknowledgement has been made in the text to all other material used. Throughout this thesis and in all related publications I followed the "Guidelines of the Medical University of Graz on Good Scientific Practice".

Graz, August 27, 2019 *Simon Christoph Kraler eh.*

Foreword

When I was six, I remember sitting in the car next to my father heading towards the Italian border. “Dad, what keeps our car driving?” “A 2-liter combustion engine.” “What is a combustion engine?” “Well, basically it’s an engine that generates energy by burning fuel. It’s very similar to steam engines. The combustion of petrol or gas increases the pressure within the engine which leads to mechanical power.” He drove aside, turned off the engine and took a pen to draw a schematic illustration which helped me to understand the main principle behind it. When I became older I started asking more complex questions. Since knowledge was not that easily accessible as it is today, my father went to the bookshop and bought an edition of the encyclopedia published by *F. A. Brockhaus*. Honestly, I think he just felt plagued by my relentless questioning. This period of time has been of particular importance to me as it taught me essential things about the concept of gaining knowledge. Due to the fact that *Brockhaus* was not able to answer all of my questions either, I began to question the idea of knowledge itself. “Is knowledge limited? Is science – as a tool of pure rationality – the appropriate approach to work out the world’s mysteries? Why do we believe when we could know? Will religion always has its place in our society or will it be gradually superseded by pure reason?” Although 19 years have passed I cannot answer any of these questions definitely. But what I know is that our current understanding of Mother Earth is based upon rational minds, who formulated crucial questions leading to replicable answers. So, after graduating from school and doing civilian service at the Austrian Red Cross, I decided to enroll at the Medical University of Graz. As time passed I realized that the mechanisms in our organism which keep our heart beating do not follow linear principles. Basically, there are multiple factors interacting each other that contribute to a condition we call health. The scientific term for a balanced state (e.g. health) in an open system (e.g. human beings) is called homeostasis. The findings of the Nobel Prize laureate of 2016, Yoshinori Oshumi have led to a better understanding of this state - in particular on the cellular level. Recent studies suggest that autophagy – a cellular degradation and recycling process – is necessary for functional and structural homeostasis in the heart. But if the loss of autophagy impairs cardiac Ca^{2+} handling remained unknown. In the following thesis, we tried to identify potential interactions of defective autophagy and Ca^{2+} coupling in the heart.

Acknowledgment

First, I would like to express my sincere gratitude to Simon Sedej, who gave me the chance to gain insight into cardiovascular basic research. Without your contagious enthusiasm, your ongoing support and your creative solution approaches, this thesis would not exist.

In addition, I want to thank my co-supervisor Senka Holzer, whose time I took up more than once. Your creative thinking and your profound experience with confocal imaging have been crucial for the completion of this scientific work.

Additionally, I would like to thank Mahmoud Abdellatif for the support provided. Your long-term experience in terms of statistics and programming has been of tremendous help.

I would also like to express thanks to Viktoria Herbst and Marlene Agreiter, whose assistance has been of vast importance for the preparation of the experiments performed.

Besides, I am genuinely grateful that I had the chance to apply for a student research fellowship awarded by the Medical University of Graz. The financial support provided allowed me to present parts of this work at *Heart Failure 2018 & World Congress on Acute Heart Failure* in Vienna, at the *Annual Meeting of the Austrian Heart Association 2018* held in Salzburg and at the *Annual Meeting of the German Cardiac Society 2019* in Mannheim.

Finally, I want to thank all the people in my private sphere whose support I can always count on. Special thanks to my beloved parents for their continuous support and encouragement. Many thanks to my brother-in-law Philippe Kruschitz for the stylistic suggestions made, to my better half Anna Ebner for your never-ending patience and benignity and finally many thanks to Martin Wernhart and Rui Adão for the technical assistance while experiment conduction.

Table of Content

Nonstandard Acronyms and Abbreviations

Akt	Protein kinase B
AM	Acetoxymethyl ester
AMPK	AMP-activated protein kinase
AP	Action potential
AC	Adenylyl cyclase
AGTR1	Angiotensin-II receptor type 1
AGTR2	Angiotensin-II receptor type 2
Atg5	Autophagy-related gene 5
ATP	Adenosine triphosphate
ß-AR	ß-adrenergic receptor
Ca^{2+}	Calcium ion
$[Ca^{2+}]_{cyt}$	Cytoplasmic Ca^{2+} concentration
$[Ca^{2+}]_i$	Intracellular Ca^{2+} concentration
$[Ca^{2+}]_{nuc}$	Nucleoplasmic Ca^{2+} concentration
CAFF	Caffeine
CaM	Calmodulin (calcium-modulated protein)
CaMKII	Ca^{2+}/calmodulin-dependent kinase II
CaMKKβ	Ca^{2+}/calmodulin-dependent protein kinase kinase-β
cAMP	Cyclic adenosine monophosphate
CAMTA	Calmodulin-binding transcriptional activator
CaN	Calcineurin
CaSR	Calcium sensing receptor
CCB	Calcium channel blockers
CICR	Calcium-induced calcium release
cPKC	Catalytic domain of PKCα
CREB	cAMP response element binding protein
DMSO	Dimethyl sulfoxide
DT50	Decay time of 50% amplitude
ECC	Excitation-contraction coupling
ER	Endoplasmic reticulum

ETC	Excitation-transcription coupling
FoxO1	Forkhead box protein O1
G_s	GTP-binding protein (G_s)
HDAC4	Histone deacetylase 4
IGF-1	Insulin-like growth factor 1
IP_3	Inositol trisphosphate
IP_3R	Inositol trisphosphate receptor
IRS1	Insulin receptor substrate 1
ISO	Isoprenaline
LAMP-2	Lysosome-associated membrane protein 2
LC3-II	Microtubule-associated protein 1 light chain 3-II
MEF2	Myocyte enhancer factor 2
MLC2a	α-myosin light chain
mTOR	Mechanistic target of rapamycin
Na^+	Sodium
NCX	Sodium-calcium exchanger
NFAT	Nuclear factor of activated T cells
NFκB	Nuclear factor κ B
NPC	Nuclear pore complexes
PKA	Protein kinase A
PKC	Protein kinase C
PLB	Phospholamban
RAAS	Renin-angiotensin-aldosterone system
Rheb	Ras homolog enriched in brain
RyR2	Ryanodine receptor type 2
S.E.M.	Standard error of the mean
SERCA2a	Sarcoplasmic reticulum Ca^{2+}-ATPase 2a
SR	Sarcoplasmic reticulum
SRF	Serum response factor
TFEB	Transcription factor EB
TTP	Time-to-peak

List of Figures

List of Tables

Abstract

Background: Macroautophagy (hereafter referred to as autophagy) is a cytoprotective process essential for the maintenance of cardiac structure and function. Mice lacking *Atg5*-dependent autophagy develop profound left-ventricular dysfunction, which goes along with increased susceptibility to ß-adrenergic stimulation. In cardiac myocytes perturbations of subcellular calcium (Ca^{2+}) handling are causally involved in hypertrophic gene program activation and, thus, may accelerate the development of heart failure.

Aim: We aimed to elucidate whether loss of cardiac autophagy causes impaired subcellular Ca^{2+} cycling early in life, specifically during ß-adrenergic stress and increased workload. Such early alterations of intracellular Ca^{2+} handling may contribute to the development of contractile impairment and to accelerated remodeling of cardiomyocytes with inhibited autophagy.

Methods: Left ventricular myocytes were isolated from adult (12-16 weeks old) cardiac-specific autophagy-deficient mice ($Atg5^{-/-}$) with an apparently normal phenotype and from their control littermates ($Atg5^{+/+}$) using a standard Liberase-based isolation procedure. Nucleoplasmic and cytoplasmic Ca^{2+} transients were then recorded using line-scan confocal imaging in electrically stimulated (1-4 Hz) cells loaded with Fluo-4/AM and perfused with Normal Tyrode solution containing 1 mmol/l $CaCl_2$. To assess whether subcellular Ca^{2+} homeostasis is altered in response to acute β-adrenergic stress, isolated cardiomyocytes were acutely exposed to the β-adrenergic agonist isoprenaline (10 nmol/l). After each experiment, high-dose caffeine (30 mmol/l) was administered to evaluate the sarcoplasmic reticulum Ca^{2+} content.

Results: Although autophagy-deficient myocytes displayed preserved Ca^{2+} cycling under basal conditions and upon acute ß-adrenergic stimulation, high-frequency pacing revealed blunted amplitudes of subcellular Ca^{2+} transients along with enhanced nucleoplasmic Ca^{2+} load, which may be an important determinant of Ca^{2+} dependent hypertrophic gene program activation.

Conclusion: The lack of *Atg5*-dependent autophagy results in early alterations of subcellular Ca^{2+} homeostasis in left ventricular cardiomyocytes. Our results suggest that reinstating basal autophagy preserves rapid changes of the intracellular Ca^{2+} handling upon

stress and conditions of increased workload, and may, therefore, attenuate hypertrophic remodeling and protect from heart failure.

Zusammenfassung

Hintergrund: Makroautophagie (im Folgenden als Autophagie bezeichnet) ist für die strukturelle sowie funktionelle Homöostase des Herzens essentiell. Mäuse mit defekter *Atg5*-abhängiger Autophagie entwickeln eine hypertrophe linksventrikuläre Dysfunktion, welche mit erhöhter Suszeptibilität gegenüber β-adrenerger Stimulation einhergeht. Rezente Studien legen nahe, dass Störungen der subzellulären Kalzium (Ca^{2+}) Homöostase ventrikulärer Kardiomyozyten in der Regulation Hypertrophie-assoziierter Gene eine zentrale Rolle spielen und damit mit der Genese der Herzinsuffizienz kausal verbunden sind.

Ziel: Wir haben untersucht, ob Autophagie-Defizienz früh im Leben mit einer gestörten Ca^{2+} Homöostase assoziiert ist. Derart frühe Veränderungen der intrazellulären Ca^{2+}-Regulation kann zur Entwicklung kontraktiler Dysfunktion und verstärktem Remodeling in Autophagie-defizienten Kardiomyozyten beitragen.

Methoden: Linksventrikuläre Kardiomyozyten wurden von Autophagie-defizienten Mäusen (*Atg5*$^{-/-}$, 12-16 Wochen) und ihrer Kontrollgruppe (*Atg5*$^{+/+}$) unter Anwendung eines Liberase-basierten Isolationsprotokolls gewonnen. Anschließend erfolgte die Beladung mit dem Ca^{2+}-sensitiven Farbstoff Fluo-4/AM, woraufhin unter Perfusion mit Normal Tyrode (1 mmol/l $CaCl_2$) zyto- sowie nukleoplasmatische Ca^{2+}-Transienten elektrisch stimulierter Kardiomyozyten (1-4 Hz) mittels Konfokalmikroskop aufgezeichnet wurden. Um in Autophagie-defizienten Myozyten potenzielle Alterationen der β-adrenergen Effekte auf die Ca^{2+}-Homöostase zu studieren, wurden diese mit dem β-Agonisten Isoprenalin (10 nmol/l) stimuliert. Im Anschluss erfolgte eine Hochdosis-Koffein-Applikation (30 mmol/l), um den intrazellulären Ca^{2+} -Speicher zu erfassen.

Ergebnisse: Obschon *Atg5*-defiziente Myozyten eine erhaltene subzelluläre Ca^{2+} Homöostase unter basalen Bedingungen sowie akutem β-adrenergem Stress zeigten, konnten wir bei Kardiomyozyten mit defekter *Atg5*-abhäniger Autophagie abgeschwächte Amplituden sowie eine erhöhte nukleoplasmatische Ca^{2+} Konzentration unter Hoch-Frequenz-Stimulation feststellen, welcher eine bedeutende Rolle in der Ca^{2+} abhängigen Transkriptionsregulation zukommen könnte.

Diskussion: Der Verlust *Atg5*-abhängiger Autophagie resultiert in früh feststellbaren Alterationen der subzellulären Ca^{2+} Homöostase linksventrikulärer Kardiomyozyten. Aus

dieser Studie lässt sich ableiten, dass die kardiale Autophagie für die Präservation der intrazellulären Ca^{2+} Homöostase unter Stress (i.e. Hoch-Frequenz-Stimulation) essentiell ist und damit in Hinblick auf die Regulation Hypertrophie-assoziierter Gene eine protektive Rolle einnehmen könnte.

1 Introduction

1.1 Overview

Macroautophagy (hereafter referred to as autophagy) has been recognized as an essential cellular process that maintains the structure and function of virtually every organ, including the heart (Choi *et al.*, 2013). Specifically, autophagy is a cytoprotective mechanism, which degrades and recycles dysfunctional cytoplasmic components such as damaged organelles and long-lived, potentially toxic proteins, lipids and other molecules (Yin *et al.*, 2016). Numerous studies have reported that the autophagic flux in the heart declines with aging (Terman, 1995; Taneike *et al.*, 2010; Cuervo *et al.*, 2005; Donati *et al.*, 2001). For example, mice lacking cardiac-specific *Atg5*-dependent autophagy develop profound left ventricular dysfunction, which goes along with increased cardiomyocyte death upon chronic ß-adrenergic stimulation, resulting in an early onset of fulminant heart failure (Taneike *et al.*, 2010; Nakai *et al.*, 2007), which might be partly related to the aberrant calcium (Ca^{2+}) homeostasis due to impaired autophagy. That being said, it has become increasingly evident that perturbations of intracellular Ca^{2+} cycling are causally involved in hypertrophic gene program activation and, thus, may accelerate the development of heart failure (Sedej *et al.*, 2014; Ljubojevic *et al.*, 2014). Recently, it has been also demonstrated that the autophagic flux in the heart is partly regulated by intracellular Ca^{2+} (Shaikh *et al.*, 2016). Whether reduction or complete loss of *Atg5*-dependent autophagy, however, is associated with disturbed Ca^{2+} handling machinery remains unknown. To this end, this study aimed to identify potential alterations of intracellular Ca^{2+} homeostasis in autophagy-deficient mouse cardiomyocytes under basal conditions at different pacing frequencies and during acute ß-adrenergic stress.

1.2 Ca^{2+} signaling and its regulation of gene expression

In eukaryotic cells, Ca^{2+} plays an important role in various cellular functions, including proliferation, differentiation, motility, secretion, apoptosis and neuronal plasticity (Dewenter *et al.*, 2017). In cardiac myocytes (excluding the pacemaker cells), Ca^{2+} is indispensable for the generation of every single contraction (Ringer, 1883) and, thus enables the heart to beat regularly and to pump blood into the systemic vasculature according to the body's demands, from early stages in embryonic development to

advanced age. If we consider a heart rate of 75 beats per minute, the human heart contracts 108.000 times every day, which makes together 39 million beats per year and more than 3 billion contractions in a human lifespan of 80 years. Proper heart function critically depends on the precise regulation of the rise and fall of intracellular Ca^{2+}, which is achieved by a sophisticated interplay of different proteins. Such dynamic changes of intracellular Ca^{2+} during the excitation-contraction coupling (ECC) at the level of a single cardiomyocyte, and together with several millions of other cardiomyocytes within the heart build up the contractile force to expel the blood into the vasculature (Eisner *et al.*, 2017). In the last decades, it has become increasingly evident that besides its pivotal role in cardiac ECC, intracellular Ca^{2+} also modulates gene expression in a process termed excitation-transcription coupling (ETC) (Atar *et al.*, 1995). It has been shown that Ca^{2+}-dependent transcriptional pathways and intracellular Ca^{2+} homeostasis undergo significant alterations during the development of heart failure and, thus, modulation of intracellular Ca^{2+} cycling might hold promising therapeutic potential (Bers, 2008).

1.2.1 Cardiac excitation-contraction coupling

Cardiac ECC describes the process by which an electrical stimulus, i.e. sarcolemmal action potential (AP) initiates an increase in the concentration of intracellular Ca^{2+} ($[Ca^{2+}]_i$), leading to the myofilament activation and, subsequently, resulting in cardiomyocyte contraction (Fig. 1) (Bers, 2002). Increase in $[Ca^{2+}]_i$ is triggered by an AP, which propagates in a timely highly coordinated manner from the sinoatrial node, a group of pacemaker cells located in the wall of the right atrium, via the atria, atrioventricular node, His bundle, and further along the right and left bundle branches and the Purkinje fibers to the whole ventricular myocardium. Such AP depolarizes the sarcolemma by activating voltage-activated sodium (Na^+) channels and subsequently opening voltage-gated L-type Ca^{2+} channels (i.e. dihydropyridine receptors), which, in turn, generate inward Na^+ and Ca^{2+} currents, respectively. In ventricular cardiomyocytes, L-type Ca^{2+} channels are typically located at the junction between the sarcolemma and sarcoplasmic reticulum (SR), thereby allowing a small amount of Ca^{2+} to enter into the cytosol and trigger the bulk of Ca^{2+} release via ryanodine receptor type 2 (RyR2). The activation of these homotetrameric proteins results in a rapid rise of global $[Ca^{2+}]_i$ from 0.1 µmol/l during diastole to 1 µmol/l during systole (Bers, 2002; Bers and Guo, 2005). Such a small influx of extracellular Ca^{2+}

that brings up the release of large amounts of Ca^{2+} from the SR into the cytosol of cardiac myocytes is termed Ca^{2+}-induced Ca^{2+} release (CICR) (Fabiato, 1983). Of note, L-type Ca^{2+} channels on the sarcolemmal t-tubule membrane and RyR2 on the SR are spatially located in very close proximity (~15 nm), thereby forming functional Ca^{2+} release complexes, also termed couplons (McNutt, 1969). It has been assumed that couplons are organized in a cluster of ~75-100 RyR2 and ~10 L-type Ca^{2+} channels (Scriven *et al.*, 2010), however, more recent studies suggest an even smaller number of RyR2 being present within one couplon (Scriven, Asghari and Moore, 2013; Kohl *et al.*, 2013; Baddeley *et al.*, 2009). In this manner the opening of one L-type Ca^{2+} channel and the binding of 2-4 Ca^{2+} ions to the RyR2 are

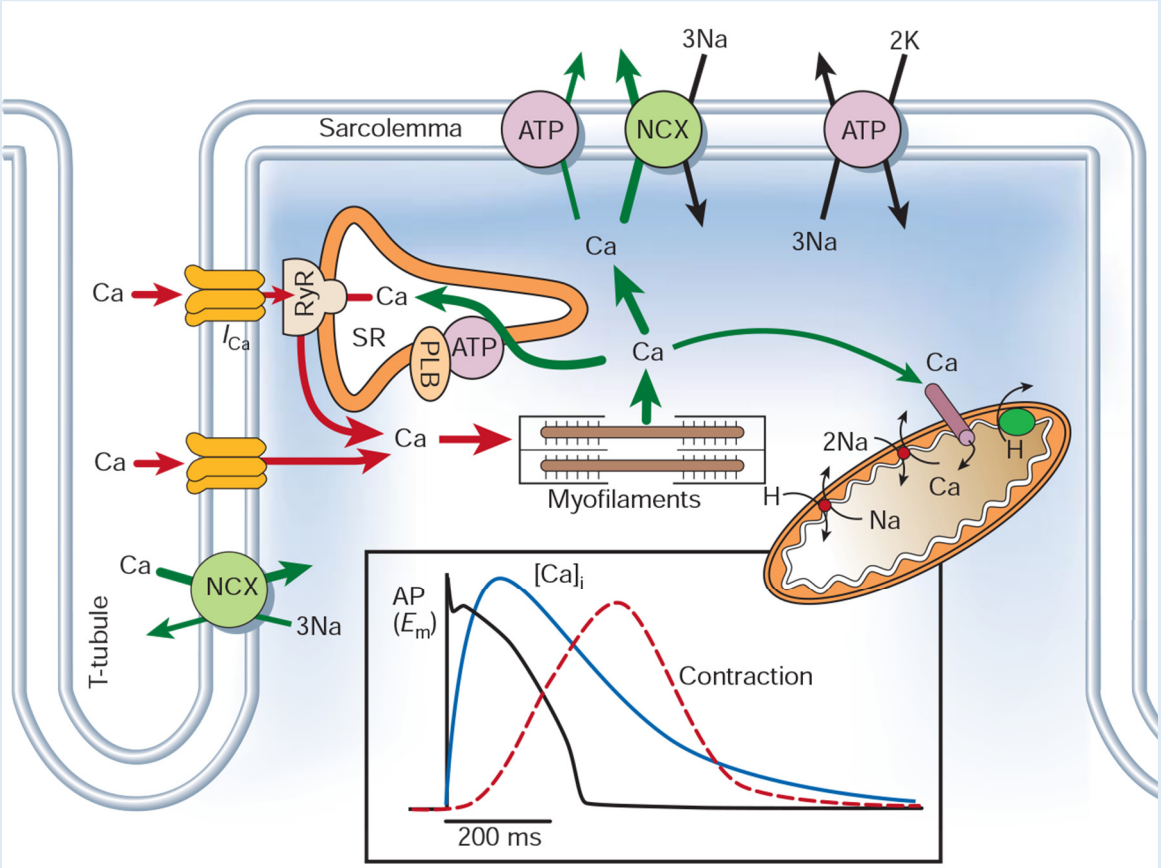

Figure 1: The process of ECC in a cardiomyocyte (adopted from Bers, 2002). Upon cell depolarization, Ca^{2+} enters ventricular myocytes through L-type Ca^{2+} channels, thereby contributing to the AP plateau. Ca^{2+}-induced Ca^{2+} release evokes a massive rise of global intracellular Ca^{2+}, thereby enabling Ca^{2+} to bind troponin C, which in turn activates the contractile apparatus. Abbreviations: AP, action potential; ATP, ATPase; $[Ca^{2+}]_i$, intracellular Ca^{2+} concentration; I_{Ca}, inward Ca^{2+} current; NCX, sodium-calcium exchanger; PLB, phospholamban; RyR, ryanodine receptor type 2; SR, sarcoplasmic reticulum.

sufficient to activate the SR Ca^{2+} release within a single couplon (Bers and Despa, 2002; Bers, 2001). Notably, the influx of extracellular Ca^{2+} through L-type Ca^{2+} channels is significantly attenuated during the SR Ca^{2+} release. The cytosolic inactivation of L-type Ca^{2+} channels is mainly initiated by the binding of calmodulin (CaM) to the carboxyl-terminus of these ion channels, thereby contributing to a significant reduction of the inward Ca^{2+} current upon the SR Ca^{2+} release (Reuter *et al.*, 1999; Peterson *et al.*, 1999; Puglisi *et al.*, 1999). This negative feedback loop is critical as it limits sarcolemmal Ca^{2+} entry and, thus, contributes to the precise regulation of the intracellular Ca^{2+} load (Bers, 2008). The activity of L-type Ca^{2+} channels is further regulated by various protein kinases, including Ca^{2+}-/CaM-dependent protein kinase II (CaMKII) as well as protein kinase A (PKA), both of which contribute to the increase in cytosolic Ca^{2+} concentration ($[Ca^{2+}]_{cyt}$) during β-adrenergic stress (Bers and Despa, 2002; Bers and Guo, 2005). It is well known that the relative contribution of RyR2-mediated versus sarcolemmal Ca^{2+} influx via L-type Ca^{2+} channels to the peak amplitude of a Ca^{2+} transient varies between species. In ventricular mouse myocytes, the RyR2-mediated *vs.* L-type-mediated contribution is 92% *vs.* 7%, while in humans, the quantitative importance of RyR2 *vs.* L-type Ca^{2+} channels is much less significant (70% *vs.* 28%) (Bassani *et al.*, 1994). The activity of RyR2 and, thus, the amount of Ca^{2+} released from the SR also underlies complex regulatory mechanisms. For example, $[Ca^{2+}]_i$ is one of the major regulators involved in modulating the RyR2-mediated Ca^{2+} release. The increase of $[Ca^{2+}]_{cyt}$ or intraluminal Ca^{2+} concentration within the SR enhances the open probability of RyR2 and, thus, provokes a rise in $[Ca^{2+}]_i$. This is observed during β-adrenergic activation, resulting in an increased amount of Ca^{2+} available for release and enhanced fractional SR Ca^{2+} release (Shannon, Ginsburg and Bers, 2000; Bassani, Yuan and Bers, 1995). Moreover, high doses of caffeine administered acutely enhances the open probability of RyR2 by Ca^{2+} sensitization and is, therefore, a useful approach to assess the SR Ca^{2+} load in experimental studies (Rousseau and Meissner, 1989). The subsequent increase in $[Ca^{2+}]_{cyt}$ is followed by a high-affinity binding of Ca^{2+} to troponin C, which initiates a cascade of events that stimulate conformational changes of the thin and thick filaments to facilitate the actin-myosin cross-bridge interaction, thereby leading to force generation, i.e. myocardial contraction (Bers, 2001). For relaxation to occur, Ca^{2+} must dissociate from troponin C and, thus, allow for conformational changes of myofilaments by disconnecting actin-myosin cross-bridges. It is important to point out that the quantity of

Ca^{2+} entering into a cardiomyocyte must be exactly the same as the amount extruded out of the cell after each cardiac cycle in order to ensure steady-state contractility (Eisner *et al.*, 2017). The main transport systems that extrude intracellular Ca^{2+} are SR Ca^{2+}-ATPase 2a (SERCA2a), sodium-calcium exchanger (NCX), sarcolemmal Ca^{2+}-ATPase and mitochondrial Ca^{2+} uniporter (Bers, 2002). However, such Ca^{2+} removal from the cytosol is largely accomplished by the reuptake of Ca^{2+} into the SR via SERCA2a and by the extrusion of Ca^{2+} through the sarcolemmal NCX. The activity of SERCA2a is essentially regulated by phospholamban (PLB), a protein that undergoes dephosphorylation or phosphorylation, resulting in the inhibition or activation of SERCA2a, respectively. For instance, phosphorylation of PLB by PKA, CaMKII or protein kinase C (PKC) causes a faster decline of intracellular Ca^{2+} and subsequently faster relaxation. Although SERCA2a competes with the sarcolemmal NCX,

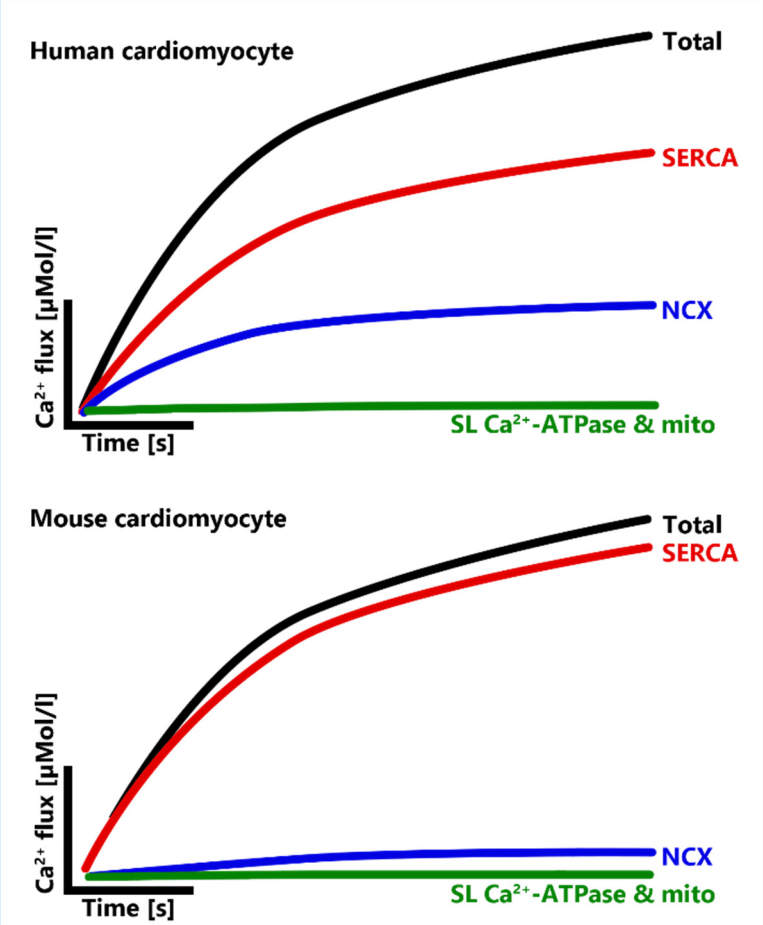

Figure 2: Differences of quantitative Ca^{2+} fluxes in mouse versus human cardiomyocytes (adopted from Bers, 2002). In healthy mouse cardiomyocytes, 92% of the cytosolic Ca^{2+} is eliminated by SERCA2a, while 7% is extruded by NCX and only 1% is removed via both the sarcolemmal Ca^{2+}-ATPase and the mitochondrial Ca^{2+} uniporter. In the human heart, however, up to 70% of cytosolic Ca^{2+} is taken up by SERCA2a, while NCX eliminates 28% of the cytoplasmic Ca^{2+}. Only 2% of the total Ca^{2} is extruded by slow transport systems, including sarcolemmal Ca^{2+}-ATPase and mitochondrial Ca^{2+} uniporter (Bers, 2002). Abbreviations: SL, sarcolemmal; mito, mitochondrial Ca^{2+} uniporter.

phosphorylation of PLB increases the SR Ca^{2+} load and, thus, enhances basal contractile function (Brittsan and Kranias, 2000). Conversely, SERCA2a is also considered to determine the velocity of cardiomyocyte relaxation and the amount of Ca^{2+} removal, which varies among different species (Bers, 2002). Of note, high heart rates in mice (~500-600 min^{-1}) are mainly due to high SERCA2a activity, which enables the myocardium to contract and relax very fast. Nevertheless, a net Ca^{2+} influx during systole must match a net Ca^{2+} efflux during diastole. Furthermore, the amount of Ca^{2+} released from the SR must also be equal to the quantity of Ca^{2+} taken up into the SR to ensure a steady-state. On the one hand, this implies that the relative contribution of NCX versus SERCA2a to Ca^{2+} removal must coincide with the L-type- *vs.* RyR2 mediated Ca^{2+} increase (Bassani *et al.*, 1994). On the other hand, species-dependent differences of the quantitative Ca^{2+} flux indicate that the amplitude of Ca^{2+} transients of mouse ventricular myocytes mainly depends on SR Ca^{2+} fluxes, whereas human cardiomyocytes are more dependent on sarcolemmal Ca^{2+} currents (Fig. 2). That being said, proper heart function depends on precise Ca^{2+} signaling at the cellular level (Luo and Anderson, 2013). In the healthy heart, cardiac output (and contractile force) is mainly regulated via three mechanisms: (1) length-dependent activation or stretch (i.e. Frank-Starling mechanism), (2) frequency-dependent activation (i.e. Bowditch effect), and (3) autonomic nervous system (e.g. ß-adrenergic stimulation). Sympathetic activation through stimulation of cardiac ß-adrenergic receptors (ß-AR) enhances contractile force (i.e. positive inotropic effect) and shortens relaxation time (i.e. positive lusitropic effect) of the myocardium (Bers, 2002; Endoh and Blinks, 1988). At the cellular level, the binding of ß-AR agonists (e.g. isoprenaline) results in the activation of the GTP-binding protein (G_s), which in turn increases intracellular cyclic adenosine monophosphate (cAMP) concentration by the activation of adenylyl cyclase (AC). High intracellular levels of cAMP subsequently activate PKA, resulting in the phosphorylation of various proteins involved in ECC, including L-type Ca^{2+} channels, RyR2, PLB and Troponin I (Fig. 3). The functional interaction of increased Ca^{2+} influx through L-type Ca^{2+} channel phosphorylation and elevated SR Ca^{2+} load due to phosphorylation of PLB results in a greater availability of intracellular Ca^{2+}, leading to higher Ca^{2+} transient amplitudes and, thus, force generation. ß-adrenergic activation further accelerates the SR Ca^{2+} reuptake by PLB phosphorylation, which is reflected by a reduced Ca^{2+} transient decay time (Endoh and Blinks, 1988). However, ß-adrenergic stimulation is not only implicated in Ca^{2+} transient amplitude

augmentation and decay time reduction, but it also modifies myofilament Ca^{2+} sensitivity (Bers, 2002). Bearing in mind that cardiac myofilaments are subjected to dynamic changes of their binding properties to troponin C under physiological conditions (e.g. acute ß-adrenergic stress), it is not surprising that myofilament Ca^{2+} sensitivity actively regulates intracellular Ca^{2+} homeostasis and cardiomyocyte contractile function.

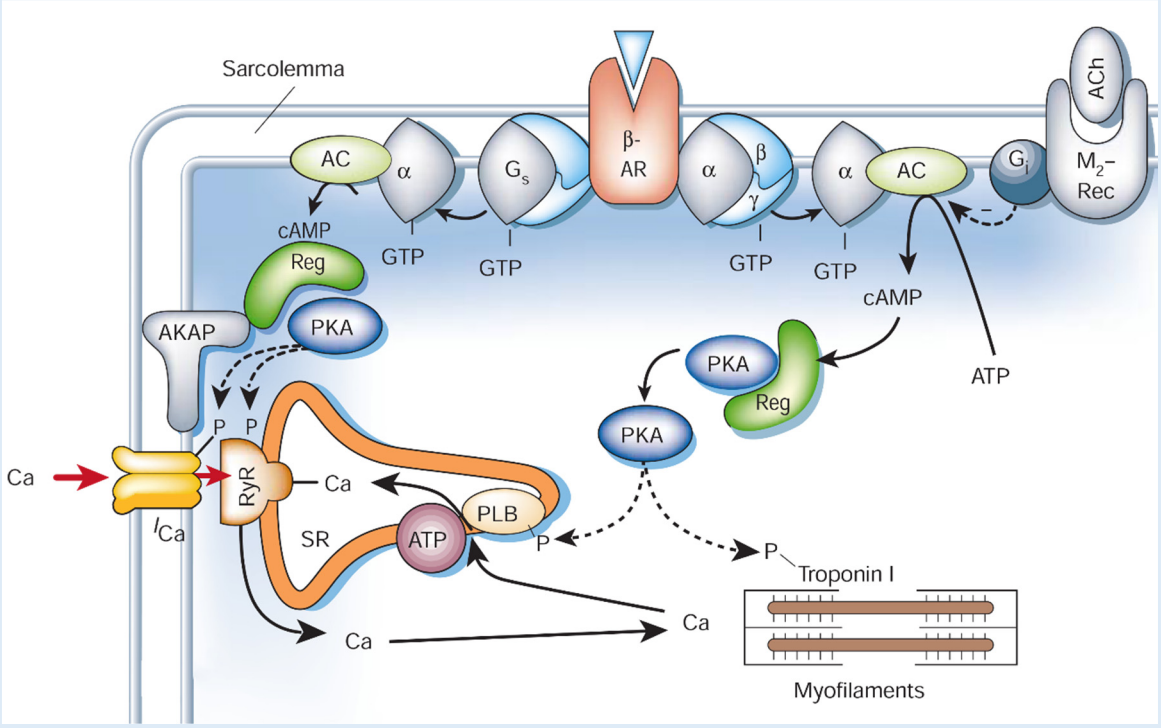

Figure 3: The effects of ß-adrenergic stimulation on ECC in cardiac myocytes (adopted from Bers and Despa, 2002). The binding of a ß-AR agonist (blue triangle; e.g. isoprenaline) activates AC, thus increasing intracellular cAMP concentration, which leads to the stimulation of PKA. PKA activation results in the phosphorylation of different proteins involved in ECC, including L-type Ca^{2+}-channels, RyR2s, PLB and Troponin I. For details, see text. Ach, acetylcholine; AKAP, A kinase anchoring protein; ß-AR, ß-adrenergic receptor; I_{Ca}, inward Ca^{2+} current; M_2-Rec, M_2-muscarinic receptor; PLB, phospholamban; PKA, protein kinase A; Reg, PKA regulatory subunit; RyR, ryanodine receptor; SR, sarcoplasmic reticulum.

1.2.2 Excitation-transcription coupling

Besides its pivotal role in directly regulating cardiac contractility, Ca^{2+} also acts as a key signal and second messenger, which shapes cardiac gene programming. The process in which signaling pathways involved in ECC exhibit transcriptional regulation is termed ETC (Anderson, 2012). The downstream mechanisms underlying ETC are not only necessary to maintain cardiac structure and function, but they are also involved in the pathogenesis of several cardiac diseases, including cardiac remodeling and heart failure (Bers, 2008; Frey, McKinsey and Olson, 2000). Although recent years have seen considerable progress in our understanding how these pathways interact with each other, and which factors contribute to the failure of cardiomyocytes, we are only at the beginning to understand how Ca^{2+}-dependent signaling pathways modify cardiac gene expression. That being said, some of the transcriptional regulators that are activated upon binding with Ca^{2+} are present in both the cytoplasm and nucleus, raising the possibility that cytoplasmic as well as nucleoplasmic Ca^{2+} may play a role in regulating cardiac gene expression. Indeed, it has been shown that disturbed *cytoplasmic* Ca^{2+} handling is associated with contractile dysfunction and the development of heart failure (Hasenfuss and Pieske, 2002). However, early alterations of *nucleoplasmic* Ca^{2+} homeostasis in failing and hypertrophied hearts (Ljubojevic *et al.*, 2014) indicate that nucleoplasmic Ca^{2+} handling may be an even more important determinant in the regulation of cardiac gene expression and, thus, causing myocardial remodeling (Ljubojevic and Bers, 2015). In cardiac myocytes, the nucleus is enclosed by two phospholipid bilayers (i.e. nuclear envelope, NE), which harbor nuclear pore complexes (NPC) that allow small ions (e.g. Ca^{2+}) to diffuse passively between the cytoplasm and nucleoplasm. Hence, each cytoplasmic Ca^{2+} transient evokes a nucleoplasmic Ca^{2+} transient, whose distinct kinetics mainly result from its passive nature but is — at least in part – modulated by mechanisms independent from the $[Ca^{2+}]_{cyt}$ (Kockskamper *et al.*, 2007; Ljubojević *et al.*, 2011). Notably, the NE does not only surround the nucleus and, thus, encapsulates the genome, but it also functions as a perinuclear Ca^{2+} store, which has been shown to be closely involved in the regulation of nucleoplasmic Ca^{2+} transients (Mauger, 2012). Ca^{2+}-dependent transcriptional pathways that modify cardiac gene expression and, thus, may contribute to the adverse structural and functional remodeling of the diseased heart are well-characterized and outlined in Figure 4. For example, CaM is a versatile intracellular Ca^{2+} sensor protein that exerts highly differentiated effects on

cardiac gene expression via activation of CaM-binding transcriptional activator (CAMTA), CaMKII or calcineurin (CaN) (Dewenter *et al.*, 2017; Finkler, Ashery-Padan and Fromm, 2007). In the nucleus, the binding of CAMTA to the homeobox protein NKX2-5 has been shown to activate genes associated with pathological remodeling in the heart (Dewenter *et al.*, 2017). Like CAMTA, CaMKII – a serine/threonine protein kinase – is also stimulated upon binding with Ca^{2+}/CaM and, thus, represents an important Ca^{2+}-dependent transcriptional regulator in the heart (Bers, 2011). Besides its central role in cardiac remodeling through transcriptional regulation, CaMKII is also implicated in the modification of chromatin-structure (e.g. phosphorylation of H3S10) (Awad *et al.*, 2013) and activation of specific proteins involved in the structural modification of chromatin, such as Histone deacetylase 4 (HDAC4; Lehmann *et al.*, 2014). An emerging body of evidence has further demonstrated the central role of the CaMKII-dependent activation of nuclear factor κ B (NFκB) during inflammatory processes, including ischemia-reperfusion injury (Gray CB *et al.*, 2017). As stated above, CaM is also involved in the activation of CaN-dependent signaling pathways. CaM-CaN interaction initiates a cascade of events coupled to hypertrophic signaling mainly via the CaN-mediated dephosphorylation of nuclear factor of activated T cells (NFAT) and, thus, stimulation of NFAT (Bueno *et al.*, 2002). Thereby, cytosolic NFAT is translocated into the nucleus, where it activates transcription of genes related to hypertrophic growth. However, nucleoplasmic NFAT can also be activated directly by CaN upon its translocation from the cytosol into the nucleus through nuclear pores. The involvement of CaN dependent signaling pathways in both cardiac development and hypertrophic remodeling processes has been demonstrated in multiple studies (Hallhuber *et al.*, 2006; Molkentin, 2000; Xiwei Zheng, Cong Bi, Marissa Brooks, 1998). In the heart, calpain is another well-characterized player that orchestrates pathological remodeling in a Ca^{2+}-dependent manner. It exerts its effects on gene regulation via both the catalytic domain of PKCα (cPKC) and CaN-dependent activation of NFAT (Burkard *et al.*, 2005; Zhang *et al.*, 2011). Although remarkable progress has been made in understanding of Ca^{2+} dependent signaling pathways that regulate cardiac gene expression, further research is certainly needed to (1) elucidate the mechanisms that allow cardiac myocytes to distinguish between "contractile Ca^{2+}" and Ca^{2+} involved in transcriptional regulation, and (2) clarify the quantitative importance and, thus, impact of dysfunctional Ca^{2+} homeostasis on the structural and functional deterioration of the diseased heart.

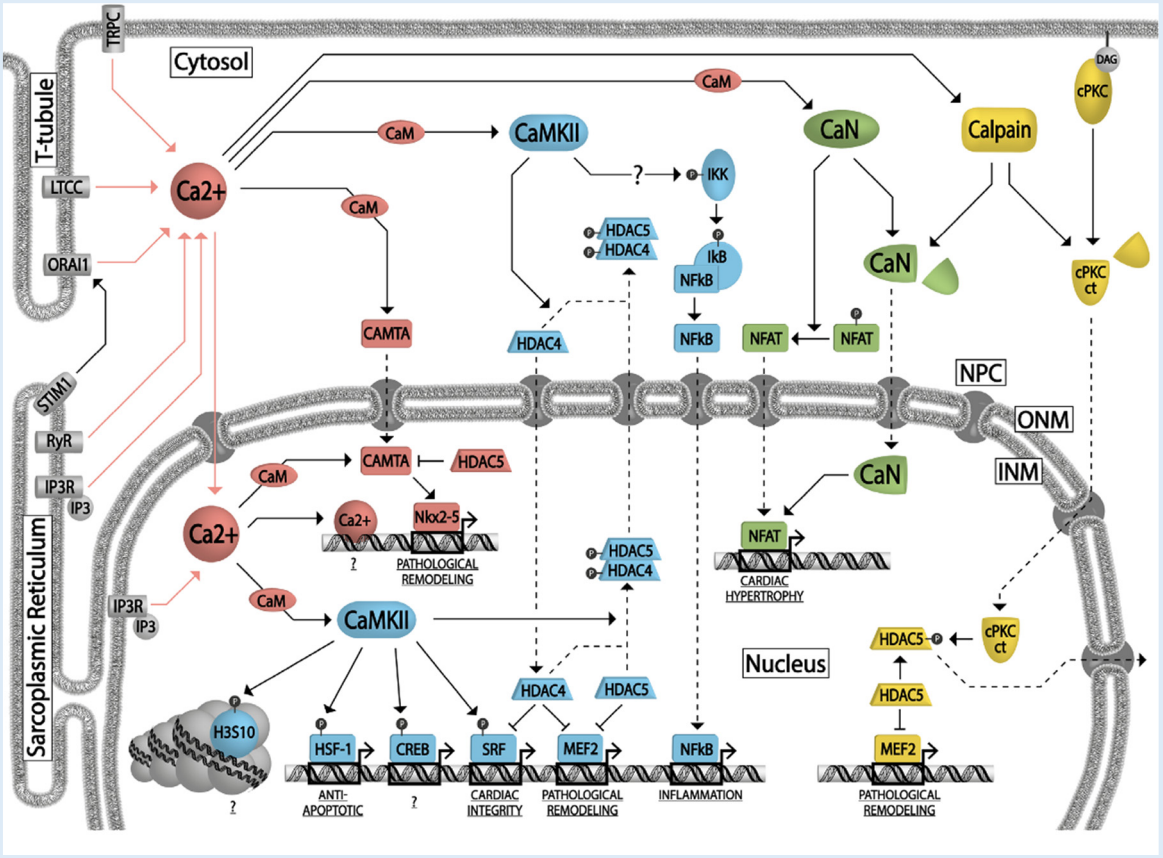

Figure 4: Gene expression regulated by Ca^{2+} in cardiomyocytes (adopted from Dewenter *et al.*, 2017). A sophisticated network underlies Ca^{2+}-dependent regulation of gene expression in cardiac myocytes. Signaling pathways involved in hypertrophic remodeling are discussed in the main text. Abbreviations: cPKCct, conventional protein kinase C c terminal; CREB, cAMP response element binding protein; DAG, diacylglycerol; H3S10, histone 3 serine 10; HSF1, heat shock factor 1; IκB, inhibitor of kappa B; IKK, inhibitor of kappa B kinase; INM, inner nuclear membrane; IP3, inositol 1,4,5-trisphosphate; IP3R, inositol 1,4,5-trisphosphate receptor; LTCC, L-type Ca^{2+} channel; MEF2, myocyte enhancer factor 2; NFAT, nuclear factor of activated T cells; NFκB, nuclear factor kappa B; NPC, nuclear pore complex; ONM, outer nuclear membrane; RyR, ryanodine receptor; SRF, serum response factor; STIM1, stromal interaction molecule 1; and TRPC, classical transient receptor potential channel.

1.2.3 Defective Ca^{2+} signaling in failing and hypertrophied hearts

Functional and structural alterations of both the intracellular Ca^{2+} handling machinery and Ca^{2+}-dependent transcriptional pathways are hallmarks of heart failure (Dewenter *et al.*, 2017). Although heterogeneous in its etiology, disease progression and clinical presentation, failing hearts display consistent molecular features associated with contractile dysfunction. Structurally, failing hearts show poorly organized t-tubule

architecture, which goes along with a reduced density of nuclear invaginations (Ljubojevic *et al.*, 2014; Horiuchi-Hirose *et al.*, 2010; Wei *et al.*, 2010). Furthermore, expression, posttranslational modification and activity states of key proteins involved in ECC (e.g., SERCA2a, RyR2, PLB) undergo significant changes during the development of heart failure with negative implications. For instance, enhanced sarcolemmal NCX activity and attenuated SERCA2a function cause augmented extrusion of intracellular Ca^{2+} from cardiomyocytes and, thus, a net reduction of the SR Ca^{2+} content. Chronic activation of ß-adrenergic signaling further increases PKA activity, resulting in hyperphosphorylated RyR2 amongst others. The elevated phosphorylation status of RyR2 increases their open probability and subsequently leads to the characteristic SR Ca^{2+} leak during diastole (Fig. 5), thereby contributing to the SR Ca^{2+} depletion (Marks, 2013) and Ca^{2+}-triggered arrhythmias (Sedej *et al.*, 2010). Disturbed SR Ca^{2+} cycling and compromised SR Ca^{2+} load significantly alter intracellular Ca^{2+} homeostasis as demonstrated by reduced Ca^{2+} transient amplitudes, prolonged time-to-peak (TTP) and delayed extrusion of intracellular Ca^{2+} (Lehnart *et al.*, 2009). In addition, disturbances in cytosolic Ca^{2+} during the development of heart failure are accompanied by early alterations in *nucleoplasmic* Ca^{2+} signaling, which precede perturbations of *cytoplasmic* Ca^{2+} handling (Ljubojevic *et al.*, 2014). Such disturbances in *nucleoplasmic* Ca^{2+} handling might contribute to accelerated development and progression of hypertrophy and heart failure (Ljubojevic *et al.*, 2014). Besides perturbations of intracellular Ca^{2+} cycling, failing cardiomyocytes also show significant alterations in the expression and activity of Ca^{2+}-dependent proteins involved in transcriptional regulation, including CaM, CaN and CaMKII (Dewenter *et al.*, 2017). For instance, CaMKII that is activated upon ß-adrenergic stress is overactive in failing hearts and, as reported above, is causally implicated in hypertrophy (Zhang *et al.*, 2003; Kirchhefer *et al.*, 1999). Additionally, CaN activity has been reported to be augmented in patients with compensated cardiac hypertrophy or heart failure (Haq *et al.*, 2001; Lim and Molkentin, 1999).

1.3 Autophagy in the heart

The word autophagy was coined from the Greek words *auto* and *phagein,* which means “self-eating”. Autophagy is a lysosome-mediated mechanism crucial for protein turnover, organelle degradation and the breakdown of cellular components (Shaikh *et al.*, 2016). To

date, we know three different autophagic pathways, including microautophagy, macroautophagy and chaperone-mediated autophagy (Nishida *et al.*, 2009). During microautophagy, cytoplasmic elements are directly internalized by lysosomes and undergo lysosomal degradation. In chaperone-mediated autophagy, proteins that display a KFERQ sequence bind to a chaperone (i.e. heat-shock cognate 70, HSC70) and are translocated into the lysosomal lumen for a subsequent breakdown (Orogo and Gustafsson, 2015). Macroautophagy is eventually the most prevalent type of autophagy that involves the degradation of dysfunctional and, thus, potentially toxic intracellular components. Upon phagophore elongation, cellular cargo designed for degradation is enclosed by a double-membrane structure called autophagosome that subsequently fuses with a lysosome, thereby forming autolysosome for enzymatic degradation of its content (Galluzzi *et al.*, 2014). The formation of autophagosomes critically depends on multiple genes, including *Atg5* (Fig. 6) (Shaikh *et al.*, 2016; Orogo and Gustafsson, 2015; Bravo-San Pedro *et al.*, 2017). Based on its pivotal role in quality control of proteins and organelles, autophagy is indispensable to preserve cellular and tissue homeostasis, especially during the course of aging (Shirakabe *et al.*, 2016). Autophagic degradation supplies not only energy-rich substrates for adenosine triphosphate (ATP) production and cellular synthesis of fatty- and amino acids, but is also centrally involved in the cellular response under stress conditions (e.g. deprivation of oxygen or nutrients, mechanical and metabolic stress) (Choi *et al.*, 2013; Abdellatif *et al.*, 2018; Kroemer *et al.*, 2010; Nishida *et al.*, 2009). Growing body of evidence suggests that impaired autophagy during aging results in the accumulation of dysfunctional cellular constituents (e.g., damaged mitochondria and misfolded proteins). That said, autophagy is critically involved in the pathogenesis of age-associated cardiovascular diseases, such as heart failure (Abdellatif *et al.*, 2018).

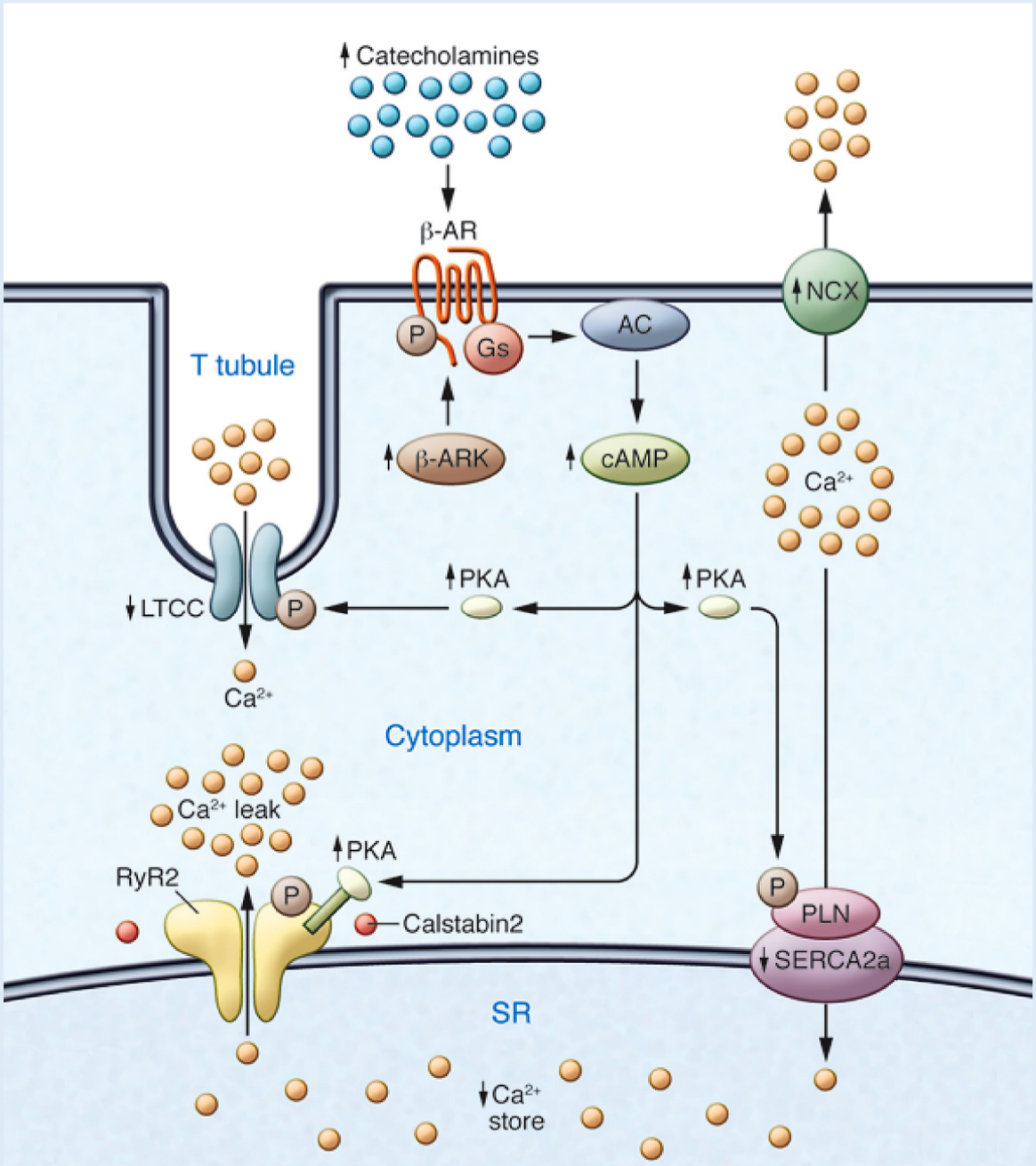

Figure 5: Altered intracellular Ca^{2+} handling in failing cardiomyocytes (adopted from Marks, 2013). In failing hearts, impaired hemodynamics due to compromised cardiac function evokes chronic stimulation of cardiac ß-AR and subsequent increased phosphorylation of various proteins (e.g. LTCC, RyR2, PLN, ß-AR), which are involved in regulating intracellular Ca^{2+} cycling. Furthermore, the expression of SERCA2a is downregulated and its activity is further compromised by reduced phosphorylation of PLN. Additionally, NCX activity and expression are augmented in failing cardiac myocytes. AC, adenylyl cyclase; ß-AR, ß-adrenergic receptor; ß-ARK, ß-AR kinase; LTCC, L-type Ca^{2+} channel; NCX, sodium-calcium exchanger; PKA, protein kinase A; PLN, phospholamban; RyR2, ryanodine receptor type 2; SERCA2a, SR Ca^{2+}-ATPase 2a; SR, sarcoplasmic reticulum.

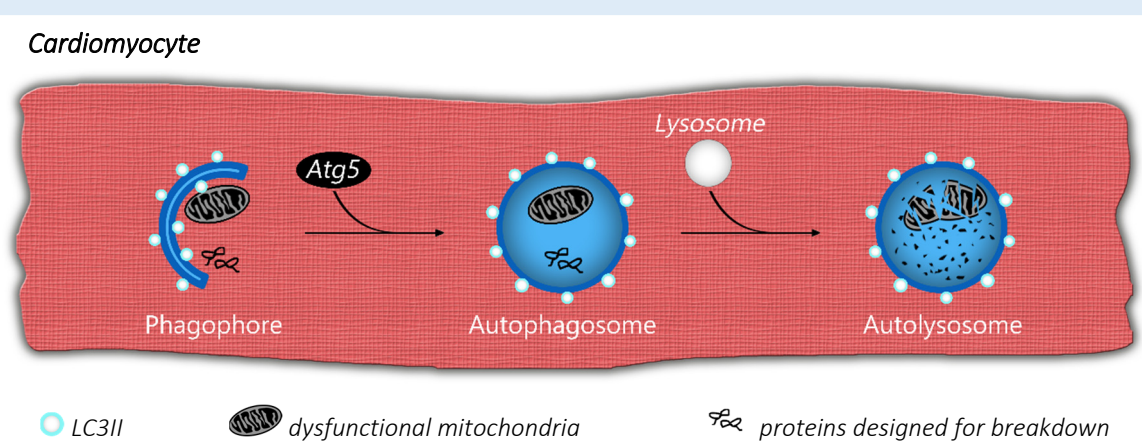

Figure 6: Autophagy in the heart. Macroautophagy is characterized by the formation of phagophores, which sequester damaged organelles and long-lived, aberrant proteins into autophagosomes. These steps critically depend on different autophagy-related proteins, including *Atg5*. Upon fusion of autophagosome with lysosome into autolysosome, the cytoplasmic cargo undergoes degradation and is recycled for new building components or energy-rich metabolites.

1.3.1 The autophagic machinery

The autophagic mechanism comprises three steps, including initiation, elongation and maturation/fusion (Fig. 7). During initiation, which is considered to be the first step of autophagy, the isolation membranes are generated, forming so-called phagophores. The exact origin of these membranes is still a matter of an ongoing debate, but accumulating evidence points toward the endoplasmic reticulum (ER), sarcolemma or mitochondria (Woodall and Gustafsson, 2018; Ge *et al.*, 2017; Hailey *et al.*, 2010; Morozova *et al.*, 2015). During the initiation process, the unc-51-like autophagy-activating kinase 1 (ULK1) is considered to be a key regulator, which initiates the activation of a protein complex, consisting of Vps15, Beclin1, and Vps34, resulting in phagophore nucleation. During the second step (i.e. elongation), the phagophore elongates. This process relies on various autophagy-related genes (e.g. *Atg5*) and during which the two-step conversion of microtubule-associated protein 1-light chain 3 (LC3) to microtubule-associated protein 1-light chain 3-II (LC3-II) occurs. LC3-II is then incorporated into the inner and outer phagophore membrane, leading to the formation of autophagosomes (Woodall and Gustafsson, 2018). Cellular levels of LC3-II can be used as a surrogate marker for

autophagosome formation and are, therefore, a widely used parameter to monitor autophagic activity (Tanida *et al.*, 2008). During the third step called maturation/fusion, autophagosomes move along microtubules through the cytosol to fuse with lysosomes, wherein the autophagic cargo undergoes hydrolases-based enzymatic degradation.

1.3.2 Cellular signals underlying autophagy regulation

Autophagy is regulated by signaling mechanisms, including mechanistic target of rapamycin (mTOR), sirtuins, growth hormone (GH)/insulin-like growth factor 1 (IGF-1) and AMP-activated protein kinase (AMPK). The serine/threonine-protein kinase mTOR is implicated in the downstream signaling of IGF-1-, sirtuin- and AMPK-dependent pathways. The activation of mTOR (e.g. induced by growth factors) results in blocked autophagy via

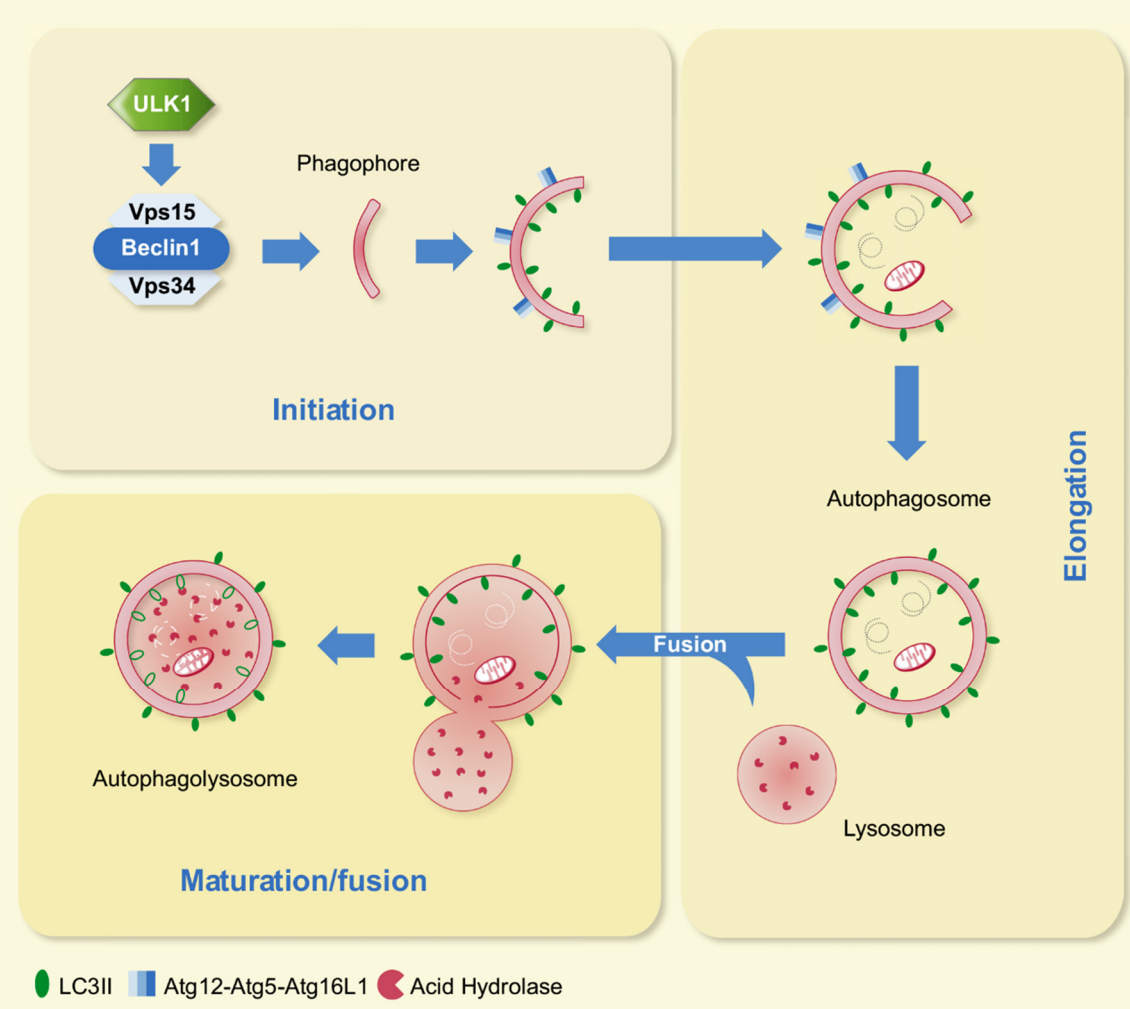

Figure 7: Simplified overview of the autophagic machinery (adopted from Woodall and Gustafsson, 2018). The autophagic pathway involves three steps: initiation, elongation and maturation/fusion. For details see main text. Abbreviations: ULK1, Unc-51 like kinase 1.

phosphorylation of ULK1 (Fig. 8), while inhibition of mTOR (e.g. induced by starvation) accelerates the autophagic flux. Inhibition of mTOR induced by rapamycin, a widely used immunosuppressant, has been shown to promote longevity in various model organisms. That said, autophagy activation mediated by mTOR-inhibition is considered to be, at least partly, responsible for its life-extending effects (Woodall and Gustafsson, 2018; Johnson *et al.*, 2013). Sirtuins (SIRT1-7) belong to a family of nicotinamide adenine dinucleotide (NAD^+)-dependent proteins critically involved in various cellular processes, such as aging, transcriptional regulation, and energy-sensing. Sirtuins are located in the cytoplasm, nucleus, and mitochondria and are implicated in both autophagy-regulation and life-span extension (Schultz and Sinclair, 2016). For instance, caloric restriction and nutrient deprivation (e.g. during starvation) enhance the autophagic flux mainly through the Sirtuin-1-mediated deacetylation of Forkhead box protein O1 (FoxO1; Hariharan *et al.*, 2010) and many of the beneficial effects (e.g. life-span extension) of caloric restriction largely depend on SIRT1 (Haigis and Sinclair, 2010). Furthermore, the GH/IGF-1 signaling axis plays a central role in the regulation of autophagic flux. For example, it has been shown that the activation of the IGF-1/protein kinase B (Akt) pathway inhibits autophagy in cardiac myocytes (Troncoso *et al.*, 2012). Additionally, AMPK partly orchestrates the regulation of autophagy in the heart. Several routes are considered to be involved in the AMPK mediated regulation of autophagy, including inhibition of mTOR and activation of TSC1/2, ULK1, and SIRT1 (Mukhopadhyay *et al.*, 2015; Cantó *et al.*, 2009). AMPK is stimulated upon depletion of ATP due to, for instance, hypoxia or substrate deficit, which enhances the autophagic flux (Woodall and Gustafsson, 2018; Gustafsson and Gottlieb, 2009).

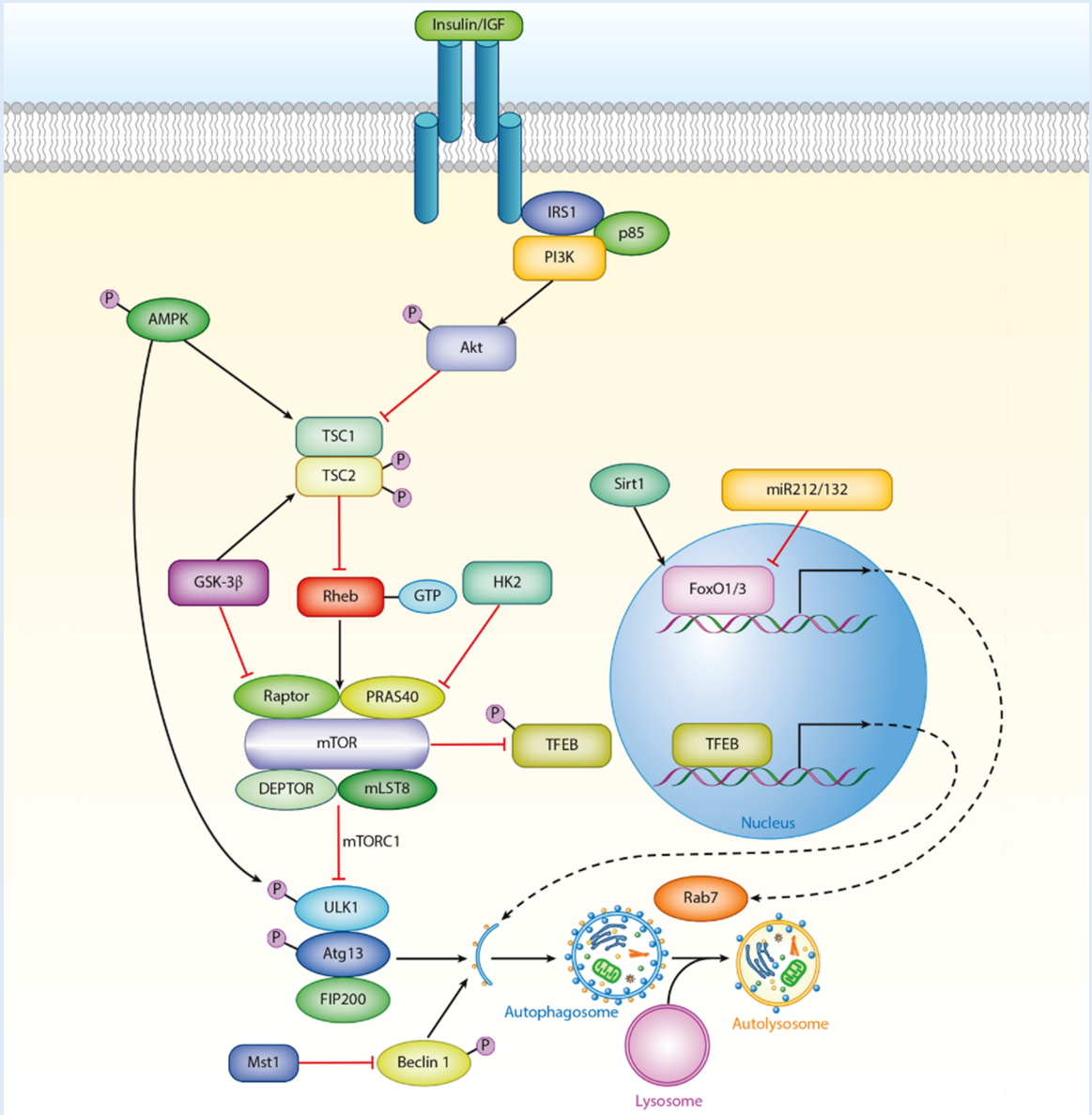

Figure 8: Schematic illustration of important signaling pathways underlying complex regulation of autophagy (adopted from Sciarretta *et al.*, 2018). Abbreviations: Akt, protein kinase B; AMPK, 5'-AMP-activated kinase; *Atg13*, autophagy-related gene 13; DEPTOR, DEP domain–containing mTOR-interacting protein; FIP200, focal adhesion kinase family-interacting protein of 200 kD; FoxO, forkhead box O; GSK-3β, glycogen synthase kinase 3β; GTP, guanosine triphosphate; HK2, hexokinase 2; IGF, insulin-like growth factor; IRS1, insulin receptor substrate 1; miR-212/132, miRNA-212/132; mLST8, mammalian lethal with SEC13 protein 8; Mst1, mammalian sterile 20-like kinase 1; mTOR, mechanistic target of rapamycin; mTORC1, mTOR complex 1; PI3K, phosphoinositide 3-kinase; PRAS40, proline-rich Akt substrate of 40 kDa; Rab7, Ras-related in brain 7; Raptor, regulatory-associated protein of mTOR complex 1; Rheb, Ras homolog enriched in brain; Sirt1, sirtuin 1; TFEB, transcription factor EB; TSC, tuberous sclerosis complex; ULK1, unc-51–like autophagy-activating kinase 1.

1.3.3 Regulation of autophagy by Ca^{2+}

Among many regulators of autophagy, Shaikh *et al*. reported that cardiac autophagy is partly modulated by intracellular Ca^{2+}. Although the ULK1-dependent autophagy initiation and phagophore nucleation are stimulated by Ca^{2+}, the phagophore elongation and

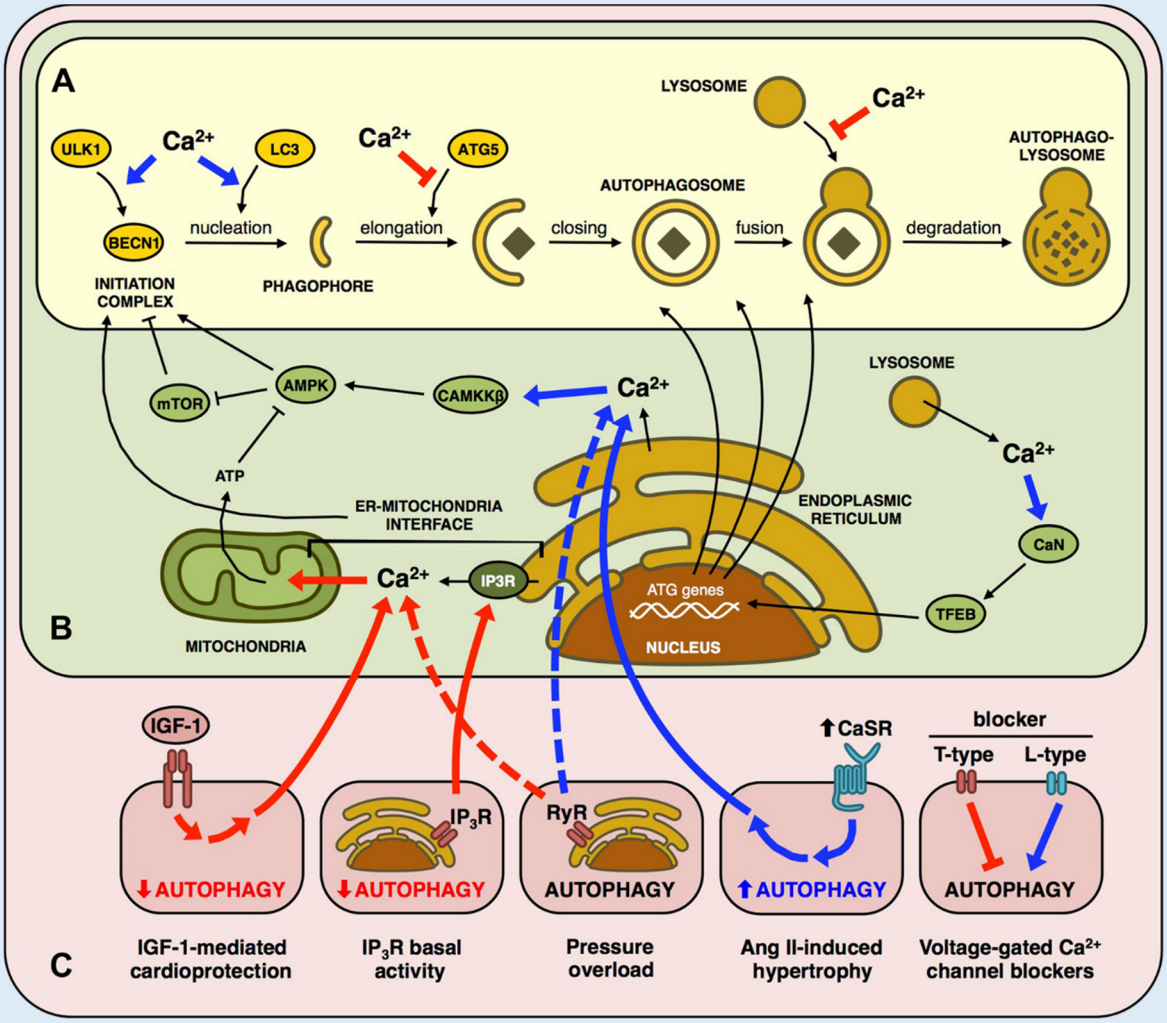

Figure 9: Autophagy in the heart and its regulation by Ca^{2+} (adopted from Shaikh *et al.*, 2016). Arrows indicate stimulatory (blue) and inhibitory (red) effects. (A) The Ca^{2+} dependent regulation of the autophagic machinery in the heart. (B) The Ca^{2+} mediated transcriptional regulation of genes involved in autophagosome-formation and its impact on autophagy initiation. (C) The role of Ca^{2+} in autophagy regulation by various signaling pathways. Abbreviations: AMPK, 5'-AMP-activated protein kinase; BECN1, beclin 1; CaMKKß, Ca^{2+}/CaM-dependent protein kinase kinase-ß; CaM, calmodulin; CaN, calcineurin; CaSR, calcium-sensing receptor; IGF-1, insulin-like growth factor I (IGF-I); IP3R, inositol trisphosphate receptor; LC3, light chain 3; mTOR, mechanistic target of rapamycin; RyR, ryanodine receptor; TFEB, transcription factor EB; ULK1, unc-51–like autophagy-activating kinase 1.

lysosomal fusion are inhibited by Ca^{2+} (Fig. 9A). On the one hand, Ca^{2+} released from the ER stimulates the formation of the initiation complex both directly via activation of Ca^{2+}/CaM-dependent protein kinase kinase-ß (CaMKKß)/AMPK and indirectly via AMPK-mediated inhibition of mTOR signaling. On the other hand, mitochondrial Ca^{2+} transfer from the ER promotes cellular synthesis of ATP, thereby blocking the AMPK pathway, which results in inhibited autophagy. In addition, lysosomal-derived Ca^{2+} stimulates transcription factor EB (TFEB), a master regulator of autophagy, that enhances the transcription of *Atg* genes, which are critically involved in autophagosome formation (Fig. 9B). Both physiological and pathophysiological stimuli differently regulate autophagy in the heart. For instance, stimulation of IGF-1 and inositol trisphosphate receptor (IP_3R) receptors is associated with reduced autophagy partly through enhanced transfer of Ca^{2+} into mitochondria. In contrast, enhanced expression of Ca^{2+}-sensing receptor (CaSR) due to angiotensin II-induced hypertrophy activates the CAMKKß/AMPK pathway, resulting in increased autophagy. Alterations in the expression of cardiac RyR2 have been reported to affect the autophagic flux both negatively as well as positively (Bround *et al.*, 2013; Zou *et al.*, 2011). Along the same line, T- and L-type voltage-gated Ca^{2+} channel blockers (CCB) also negatively and positively regulate the autophagic flux within cardiac myocytes, respectively (Fig. 9C) (Shaikh *et al.*, 2016).

1.3.4 Autophagy in cardiac disease

Several cardiac diseases, including cardiomyopathies, ischemic heart disease, ischemia-reperfusion injury, heart failure, and cardiac hypertrophy are associated with altered autophagic flux (Taneike *et al.*, 2010; Choi, Ryter and Levine, 2013; Gustafsson and Gottlieb, 2009). Furthermore, Danon disease, an x-linked metabolic disorder, is caused by a defective lysosomal membrane protein called lysosome-associated membrane protein 2 (LAMP-2; Endo *et al.*, 2015). This protein is essential for proper lysosomal function and, thus, stimulates autophagic flux as it plays a central role in the fusion of the autophagosome with the lysosome. Danon disease is characterized by the classic triad of cardiomyopathy, variable level of mental retardation and myopathy. Although the exact pathogenesis of this disease is not well understood, dysfunctional autophagy may contribute to the continuous decline in cardiac function observed in these patients (Nishino *et al.*, 2000). As mentioned above, compromised autophagic flux seems to be

tightly associated with cardiac senescence (Abdellatif *et al.*, 2018). The aged heart is characterized by increased left ventricular wall thickness, enhanced myocardial stiffness, abnormal diastolic filling pattern and chamber relaxation, which results in diastolic dysfunction (Nair and Ren, 2012; Ferrari *et al.*, 2003). Recently, it has been reported that reduced levels of autophagy are also involved in the development of diastolic dysfunction and affect the lifespan of aged C57BL/6 mice (Eisenberg *et al.*, 2016). Persistent pressure-induced overload causes maladaptive cardiac remodeling, which is characterized by ventricular dilatation, systolic dysfunction and electrophysiological alterations along with increased levels of fibrosis, resulting in life-threatening arrhythmias and pump failure (Hill and Olson, 2008). At the cellular level, increased afterload is associated with upregulated gene expression of Beclin1, which enhances the autophagic flux, accelerates pathologic remodeling and contributes to fibrotic changes in the heart (Zhu *et al.*, 2007). These findings indicate that increased levels of autophagy during the pathogenesis of afterload-induced heart failure is – at least in part - a maladaptive response (Rothermel and Hill, 2007). In contrast, pressure-induced overload in mice lacking cardiac-specific autophagy causes a profound left ventricular dilation, leading to fulminant heart failure, resulting in premature mortality (Nakai *et al.*, 2007). Bearing this in mind, it remains to be determined whether autophagy is detrimental or protective in the setting of pressure-induced overload and warrants further investigation. Besides Beclin1, the renin-angiotensin-aldosterone system (RAAS) is also involved in the modulation of autophagy during the progression of heart failure. In a rat model of cardiac hypertrophy, activation of Angiotensin II receptors type 1 (AGTR1) showed enhanced autophagic flux, while stimulation of Angiotensin II receptors type 2 (AGTR2) strongly reduced the activity of autophagy, indicating a dual modulation of cardiac autophagy (Porrello *et al.*, 2009; Steckelings and Unger, 2009). Hence, AGTR1-inhibitors may play a beneficial role in the treatment of heart failure by attenuating autophagic flux and, thus, cell death (De Meyer *et al.*, 2010). It is important to point out that increased autophagic flux is associated with ischemic heart disease. Indeed, during ischemia the blood supply to the myocardium is restrained, which results in the inhibition of mTOR signaling through the activation of AMPK (Matsui *et al.*, 2007) and subsequent autophagy induction. This suggests that reinforced autophagy seems to have an adaptive function in the ischemic heart (Valentim *et al.*, 2006). Multiple studies on rabbit, swine and rat cardiomyocytes have shown that

ischemia-reperfusion injury, which immediately occurs after the restoration of energy supply, results in massively increased autophagic flux through the activation of Beclin1 (Matsui *et al.*, 2007; Valentim *et al.*, 2006; Gurusamy *et al.*, 2009). While the induction of autophagy during ischemia exerts cardioprotective effects, the sustained upregulation of Beclin1 during reperfusion may be detrimental as it causes cardiac injury attributable to continuously high levels of autophagy (Matsui *et al.*, 2007). Another cardiac disease characterized by diminished autophagy is diabetic cardiomyopathy, a disorder that was first described in 1972 (Rubler *et al.*, 1972). These hearts typically exhibit abnormal myocardial structure and function, which manifests in the absence of coronary artery disease, valvular heart disease or other risk factors (e.g., hypertension and dyslipidemia), predisposing to the development of heart failure (Boudina and Abel, 2010). Metformin, a frequently used antidiabetic drug, activates the AMPK pathway and reinstates cardiac autophagy. Hence, metformin protects against apoptosis of cardiomyocytes and its administration may, therefore, exert beneficial effects in patients suffering from both diabetes and heart failure (He *et al.*, 2013; Andersson *et al.*, 2010; Gundewar *et al.*, 2009). Interestingly, metformin was shown to induce phospholamban degradation, resulting in increased Ca^{2+} uptake into SR (Teng *et al.*, 2015). Hence, autophagy plays a central role in maintaining not only structural and functional homeostasis of the heart, but appears to Ca^{2+} handling (Taneike *et al.*, 2010; Abdellatif *et al.*, 2018). In support of this idea, a study by Pedrozo *et al.* proposed that damaged or leaky RyR2 channels that are causally involved in the development and progression of cardiac failure (Sedej *et al.*, 2014) are likely removed through chaperone-mediated autophagy.

1.3.5 Effects of blocked autophagy on the left ventricular function under basal conditions and during ß-adrenergic stress

As less than 50% of all cardiomyocytes forming the adult heart are exchanged during a normal lifespan (Bergmann *et al.*, 2009), cellular survival mechanisms such as autophagy play a pivotal role in maintaining proper heart function during basal conditions and upon ß-adrenergic stress (Taneike *et al.*, 2010; Nakai *et al.*, 2007). Mutations that interfere with the autophagic pathway in the heart have been linked to cardiac dysfunction, accelerated cardiac aging and shortened lifespan (for details see review by Abdellatif *et al.*, 2018). At baseline, mice with cardiac-specific *Atg5* ablation – which results in blocked

autophagosome formation – develop overt cardiomyopathy marked by cardiac hypertrophy, left ventricular dilatation and contractile dysfunction, which is accompanied by increased levels of fibrosis. These alterations are accompanied by sarcomeric disarray, impaired mitochondrial structure and function, enhanced oxidative stress and augmented levels of apoptosis (Taneike *et al.*, 2010). Intriguingly, under basal conditions mice with cardiac *Atg5* deprivation do not exhibit cardiac dysfunction until the age of up to 6 months, suggesting that compensatory mechanisms protect the young heart from the detrimental consequences of blocked autophagy. Such protective mechanisms may involve degradation processes independent from *Atg5*, including chaperone-mediated autophagy and *Atg5/Atg7*-independent autophagic pathways (Taneike *et al.*, 2010). Mice with cardiac-specific *Atg5* deficiency also show increased susceptibility to chronic ß-adrenergic stress. This is exemplified by the development of contractile dysfunction and left ventricular dilatation after one-week pressure-induced overload. At the cellular level, chronic ß-adrenergic stress accelerates cardiomyocyte death, resulting in the onset of fulminant heart failure (Nakai *et al.*, 2007). These findings suggest that constitutive autophagy plays a central role in maintaining cardiac integrity and, thus, heart structure and function in the basal state and during chronic ß-adrenergic stress.

1.4 Hypothesis

Based on the vital importance of intact autophagy for structural and functional homeostasis of cardiac myocytes, we hypothesized that intracellular Ca^{2+} homeostasis is impaired in autophagy-deprived cardiomyocytes early in life. Such subclinical disturbances in Ca^{2+} handling may play a causative role in the progressive impairment of cardiac structure and function (Ljubojevic *et al.*, 2014; Sedej *et al.*, 2014). In particular, we tested whether increased stimulation frequency and/or acute β-adrenergic stress worsen Ca^{2+} cycling in autophagy-deprived cardiomyocytes.

2 Material and Methods

2.1 Mice

To test how defective autophagy affects cardiac Ca^{2+} cycling, we used cardiomyocyte-specific *Atg5* knock-out mice deficient for *Atg5*-dependent autophagy (*Atg5*$^{flox/flox}$-MLC2a-Cre^{+} mice, hereafter referred to as *Atg5*$^{-/-}$ mice). These mice have *Atg5* gene floxed out early in embryogenesis and they were generated from *Atg5*$^{flox/flox}$ mice (obtained from Riken BRC Japan, Nakai *et al.*, 2007) crossed with mice expressing Cre^{+} recombinase under the control of the cardiomyocyte-specific α-myosin light chain (MLC2a) Cre^{+} promoter (Wettschureck *et al.*, 2001). *Atg5*$^{flox/flox}$-MLC2a-Cre^{-} mice were used as controls (hereafter referred to as *Atg5*$^{+/+}$ mice). All adult mice (males and females, 12 to 16 weeks old) were housed in a 12-hour light/dark regime under specific pathogen-free conditions in the animal facility at the Institute for Biomedical Research of the Medical University of Graz with free access to standard food and water *ad libitum*.

2.2 Cell isolation

2.2.1 Work performed prior to the isolation of cardiomyocytes

All solutions were prepared (for details see appendix; Tables 1-7) and titrated with 2 mol/l NaOH to adjust pH to 7.4 at room temperature using a pH meter (pH213, Hanna Instruments, USA). Glass-bottom dishes (35 mm diameter, WillCo Wells B.V., Amsterdam, The Netherlands) were then coated with 4% laminin and incubated at room temperature for at least two hours. In the meantime, the flow rate and the temperature of a circulating water bath (LAUDA Alpha A6, Germany) was adjusted with the aim to obtain a flow rate of to 2.5 ml/min and a temperature of 37°C at the cannula tip of the Langendorff's perfusion setup (Radnoti Low Volume - High Yield Myocyte System, #120108, Radnoti, Ireland). To obtain consistent cell isolations, both flow rate and temperature at the cannula tip were measured regularly. All chemicals were purchased from Sigma-Aldrich (Vienna, Austria) unless otherwise stated.

2.2.2 Isolation of adult ventricular cardiomyocytes

Mice were lightly anesthetized in an induction chamber using isoflurane (Forane®, Baxter, USA) followed by intraperitoneal heparinization (50 I.U. heparin diluted in 0.9% NaCl solution) to prevent thromboembolism during the isolation procedure. Twenty minutes were allowed for heparin to reach all body tissues, while mice were freely moving in their cages. Mice were then again transferred to the induction chamber with 5% isoflurane, which induced deep anesthesia (ensured by a negative toe pinch test) immediately followed by cervical dislocation. The peritoneal cavity was opened beneath the costal arch and the diaphragm was dissected to expose the heart. After careful removal of the pericardium, the heart was excised at the level of the aorta and the organ was placed in a beaker containing ice-cold cannulation solution (see Table 1 for the composition) to arrest the heart and remove excessive blood. Immediately thereafter, the heart was transferred to a glass-dish containing perfusion buffer (Table 2) at 37°C as part of the Langendorff's setup and visualized using a stereomicroscope (Wild Heerbrugg M5A, Switzerland). The aorta was mounted onto the cannula using two fine-tip forceps and tightened with the surgical thread (size 5-0, Johnson & Johnson, USA) for a retrograde perfusion of the heart (Fig. 10) using a standard isolation procedure based on Langendorff's perfusion of the heart (Fig. 11) using liberase (0.075 mg/ml, Liberase™ TM Research Grade, Roche, Switzerland) and trypsin (0.056 mg/ml, GIBCO® Trypsin 2.5%, Thermo Fisher Scientific, USA) as described elsewhere (O'Connell *et al.*, 2003). The heart was perfused for ten minutes with two different solutions. Firstly, zero calcium-containing perfusion buffer was used to eliminate Ca^{2+}, thus, blocking contractions and removing any remaining blood from the coronary arteries (for 4 min). Secondly, the heart was perfused with liberase- and trypsin-containing digestion solution (Table 3) for six minutes. Then the heart was cut below the atria and both ventricles were transferred into the myocyte stopping solution 1 (Table 4), which contained bovine calf serum that inhibits the activity of proteases (O'Connell *et al.*, 2007). The left ventricle was dissected from the right ventricle and mechanically dissociated by using plastic Pasteur pipettes with sequentially reduced openings of around 3, 2 and 1 mm in diameter. We obtained a cell suspension that was filtered through a nylon-meshwork of 250 µm pore diameter and transferred into a 50 ml Falcon tube. Cardiac myocytes in the cell suspension were allowed 10 min to form a pellet by means of gravity before the supernatant was replaced every 10 min with myocyte

stopping solution 2-based solutions containing serially increased Ca^{2+} concentrations, namely 125, 250 and 500 µM, respectively (see Table 5 and 6 for solution composition). Finally, the cell pellet was resuspended in Tyrode's solution containing 1 mM $CaCl_2$ (for composition see Table 7) and cells were used for experiments.

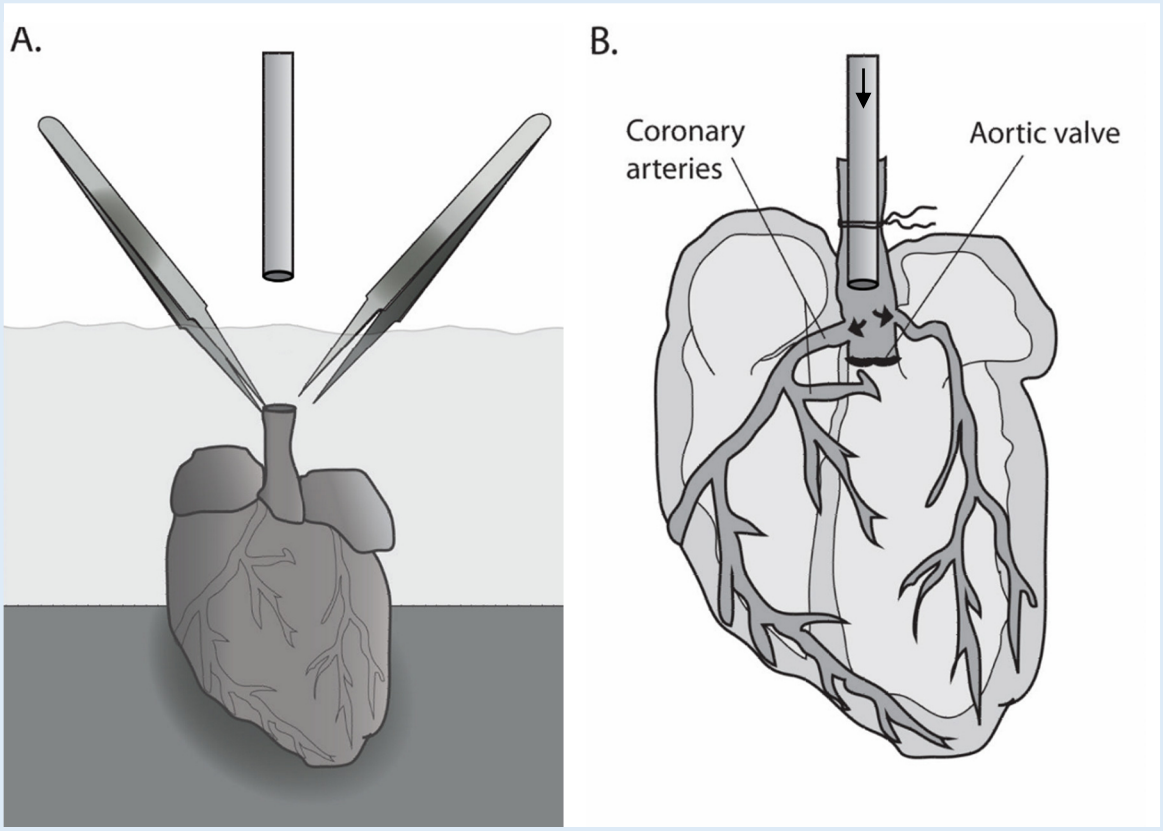

Figure 10: Schematic illustration of the aortic cannulation and the retrograde coronary perfusion (adopted from Louch *et al.*, 2011). (A) The aorta was cut at the level of the aortic arch (i.e. proximal to the brachiocephalic branch) and drawn onto the cannula using a pair of point-tip tweezers. (B) A double surgical knot prevented dislocation of the cannulated heart during the retrograde perfusion of the coronary arteries. Perfusion direction is indicated by arrow heads.

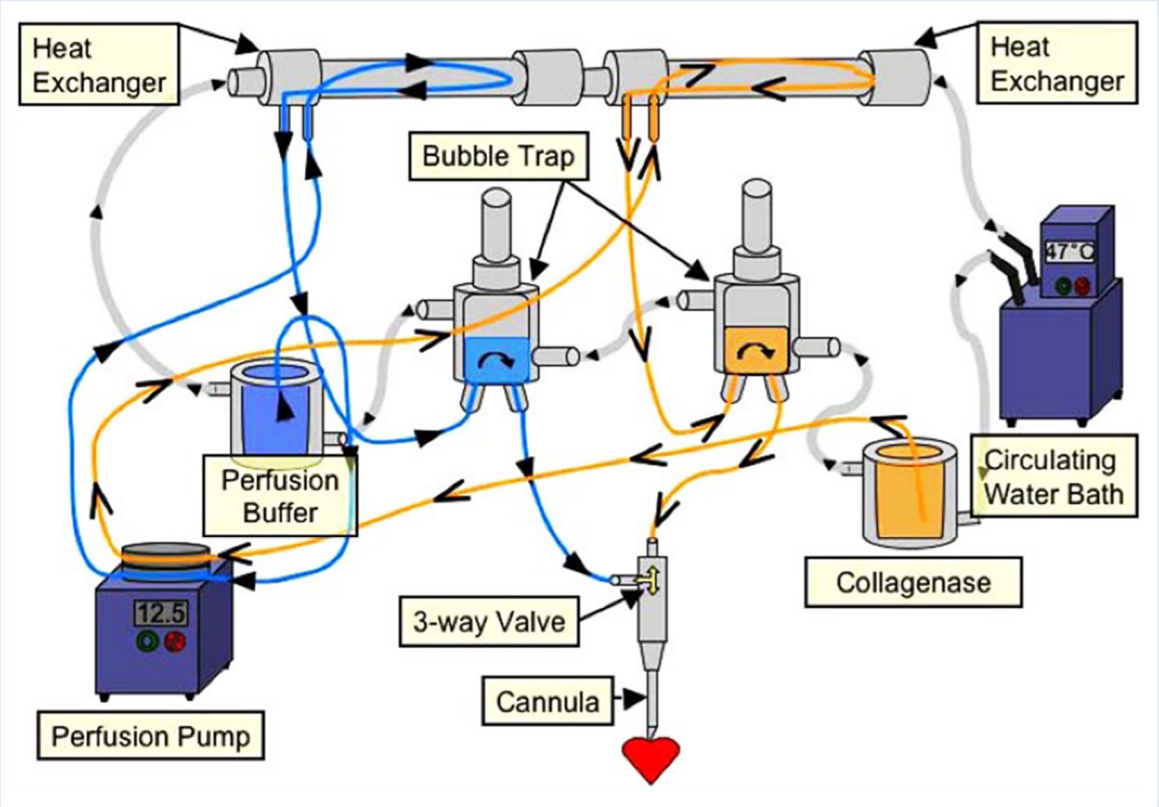

Figure 11: Scheme of Langendorff's perfusion setup (adopted from (O'Connell *et al.*, 2007). For details, see main text.

2.2.3 Loading of the Ca^{2+} fluorescent dye Fluo-4/AM into cardiomyocytes

The single-wavelength Ca^{2+} indicator Fluo-4/AM (AM, acetoxymethyl ester, Life Technologies, USA) allows measurements of $[Ca^{2+}]_i$ at both high spatial and temporal resolution (Bootman *et al.*, 2013). Upon binding of Ca^{2+} to Fluo-4/AM, the fluorescent intensity of the fluorophore is augmented by a factor of more than a hundred, which allows monitoring of relative changes in $[Ca^{2+}]_i$ in living cells (Gee *et al.*, 2000). The excitation (blue) and fluorescence emission (green) spectra upon Ca^{2+} binding are shown in Figure 12. In our experiments, freshly isolated cardiomyocytes were loaded with Fluo-4/AM dissolved in dimethyl sulfoxide (DMSO) at a final concentration of 7.8 µmol/l. Upon Fluo-4/AM enters into cardiac myocytes, the dye is hydrolyzed by esterases, which (i) reduces its lipophilic properties and, thus, its diffusion across the cell membrane, and (ii) transforms it to the Ca^{2+}-sensitive free-acid form (Bootman *et al.*, 2013). Cardiac myocytes were then plated on laminin-coated glass-bottom dishes and incubated for 40 minutes to

allow for sufficient loading with Fluo-4/AM. Fluo-4/AM that did not enter cells was removed by washing cells twice with Normal Tyrode solution.

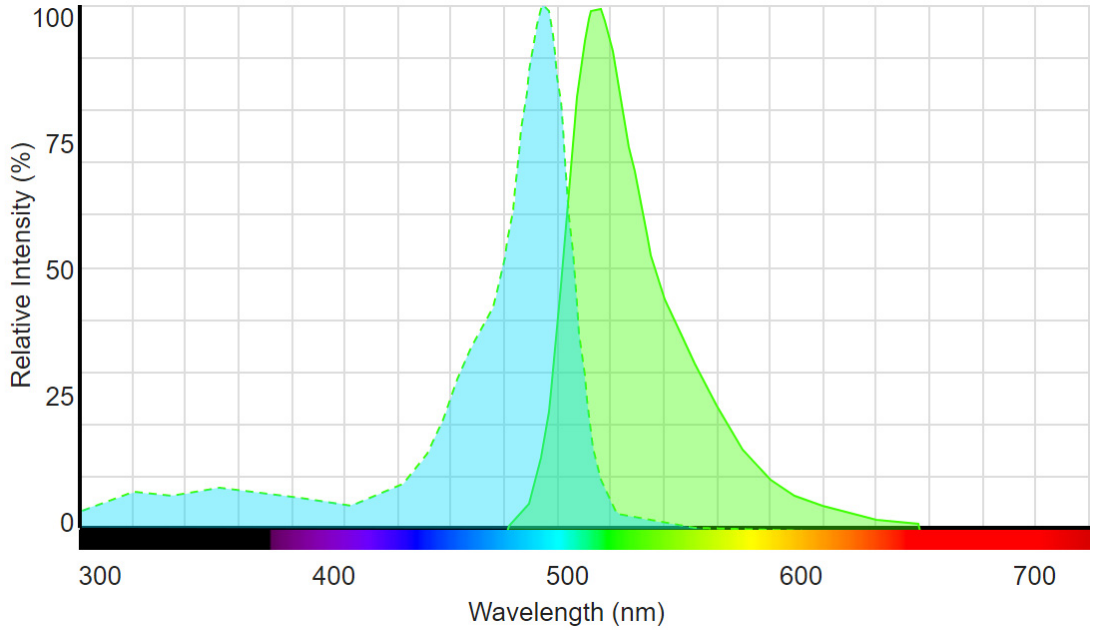

Figure 12: Spectral characteristics of Fluo-4/AM (adopted from Fluorescence SpectraViewer, ThermoFisher, 2018). Fluo-4/AM bound to Ca^{2+} shows peak excitation at a wavelength of 494 nm (blue), while its emission spectra peaks at 516 nm (green).

2.3 Confocal Microscopy

Cardiac myocytes (loaded with Fluo-4/AM) were viewed under a laser scanning confocal microscope (Zeiss LSM 700, Jena, Germany) equipped with a 40x oil-immersion objective (Fluar, numerical aperture 1.30; Zeiss, Jena, Germany). Fluo-4/AM was excited at 488 nm using an argon-ion laser (2% laser intensity, Laser Rack LSM 700, Germany), while the emitted fluorescence was acquired at wavelengths higher than 505 nm. The confocal pinhole was set to 1 Airy unit to obtain the best signal to noise ratio and to permit the in-focus light to the detector for recording in order to increase optical resolution (i.e. confocal image). Cells were perfused with Tyrode's solution using a gravity-driven superfusion pipette coupled to a valve controller (VC-8, Warner Instruments, USA) at a constant flow velocity and at room temperature. Cardiomyocytes were paced at 1 Hz using electric field stimulation (MyoPacer field stimulator, Ionoptix, Ireland) to reach a steady-state and

ensure continuously stable SR Ca^{2+} load. Steady-state Ca^{2+} transient in the cytoplasm and nucleus were acquired in a line-scan mode (512 pixels, pixel dwell time of 1.58 µs; Fig. 13). To assess the effects of acute β-adrenergic stimulation, cells were perfused with the β-adrenergic agonist isoprenaline at a concentration of 10 nmol/l. At the end of each experiment, high dose caffeine (30 mM) was rapidly administered to assess the SR Ca^{2+} load. To study frequency-dependent response, we used stimulated cells at increasing frequencies, namely 1 Hz, 2 Hz, 3 Hz and 4 Hz for 30 seconds to reach the steady-state and recorded at least 5 Ca^{2+} transients. Experiments were performed only in viable, rod-shaped, cross-striated and quiescent cardiomyocytes. The experimental protocol is depicted below (Fig. 14).

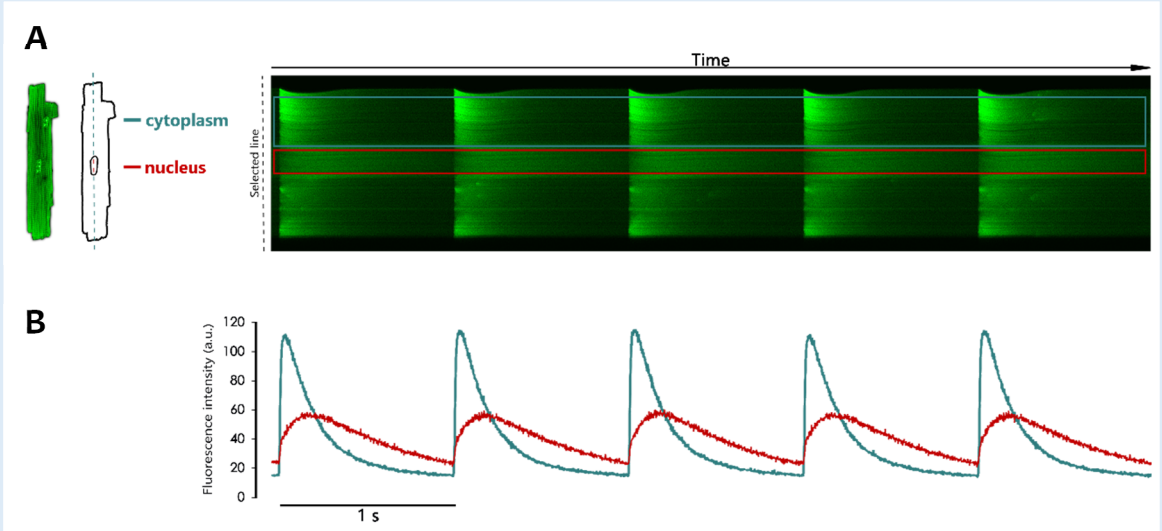

Figure 13: Representative recording of Ca^{2+} transients (cytoplasm vs. nucleus) using line-scan mode. (A) Schematic drawing of a ventricular cardiomyocyte. Fluorescence images were recorded using a 512-pixel scan-line drawn along the longitudinal-axis of electrically stimulated cardiomyocytes perfused with Tyrode's solution to record changes of $[Ca^{2+}]_i$ in the cytoplasm and nucleus. (B) Ca^{2+} transients were analyzed in the cytosol (blue trace) and nucleus (red trace) before and after the administration of 10 nM isoprenaline.

2.4 Analysis of intracellular Ca^{2+} transients

Recordings were imported to the Java-based image-processing platform ImageJ (National Institutes of Health, USA). Different regions of interest, including cytoplasm, nucleus and background were selected (Fig. 13A) and then exported into *.txt files, and converted to *.xlsx files. For steady-state Ca^{2+} transient analysis (Fig. 13B), at least five consecutive Ca^{2+}

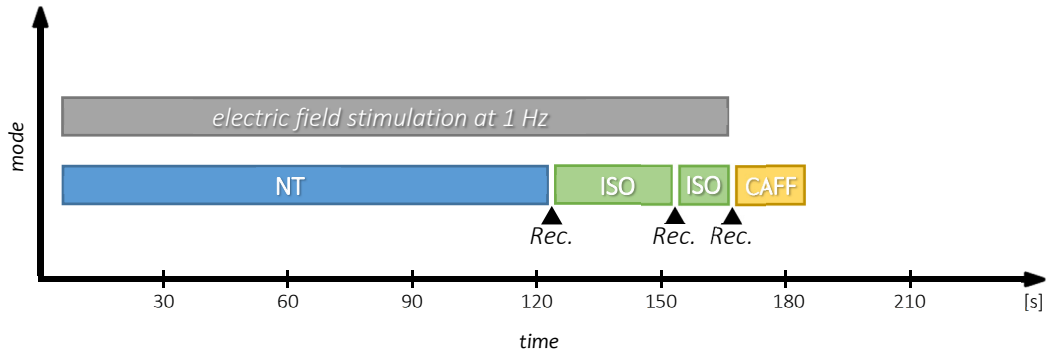

Figure 14: Experimental protocol for live-cell confocal imaging of isolated cardiomyocytes. Left-ventricular cardiomyocytes paced at 1 Hz (grey bar) were perfused with the normal Tyrode solution (NT, blue) for 120 seconds (baseline) followed by isoprenaline administration (ISO, green). At the end of each experiment, the field stimulation was then stopped and Tyrode's solution was rapidly switched to Tyrode's solution containing 30 mmol/l caffeine (CAFF, yellow) in order to assess the intracellular Ca^{2+} content released from the sarcoplasmic reticulum. To assess potential frequency-dependent alterations of subcellular Ca^{2+} homeostasis, a subset of cardiac myocytes was stimulated for 30 s at different pacing frequencies (1, 2, 3 and 4 Hz; not shown), whereupon Ca^{2+} transients were recorded. Steady-state Ca^{2+} transients were recorded (Rec., black arrow-heads) at indicated time points. The x-axis shows time.

transients were averaged using a custom-made script based on Matlab R2017a (MathWorks, USA), which is provided in the appendix. The off-line analysis of line-scan images included Ca^{2+} transient amplitudes (F/F_0), TTP and decay time of 50% relaxation from peak amplitude (DT_{50}) in the cytoplasm and nucleus (Fig. 15). The amplitude of Ca^{2+} transients was calculated following this equation:

$$F/F_0 = \frac{(F - F_{background})}{(F_{resting} - F_{background})}$$

where F is the maximum and F_0 the minimum fluorescence intensity, respectively. $F_{resting}$ is the fluorescence intensity measured in unstimulated cells, and $F_{background}$ is the fluorescence intensity determined in a region of interest adjacent to a cell. SR Ca^{2+} load was quantified as the peak amplitude of the caffeine-induced Ca^{2+} transient. To compare

β-adrenergic responsiveness between groups, relative changes (p) of Ca^{2+} transients (baseline *vs.* β-adrenergic stimulation) were calculated using the following formula:

$$p = \frac{(F/F0_{ISO} - F/F0_{NT})}{F/F0_{NT}} \times 100$$

Calibrated $[Ca^{2+}]_i$ was then derived from obtained fluorescent signals of the subcellular regions using a previously described method (Ljubojević *et al.*, 2011).

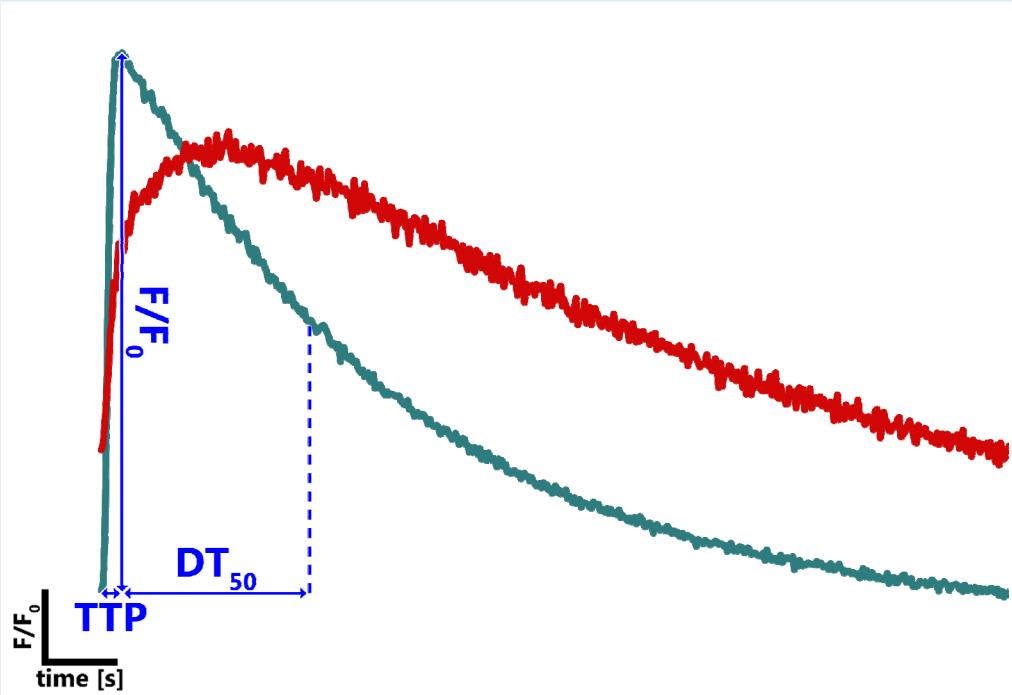

Figure 15: Analysis of Ca^{2+} transients comprised F/F_0, TTP and DT_{50}. Averaged Ca^{2+} transients were analyzed and maximum peak amplitude (F/F_0), time-to-peak (TTP) and decay time of 50% relaxation (DT_{50}) from the peak amplitude of Ca^{2+} transients were calculated in the cytoplasm (blue) and nucleus (red).

2.5 Statistical analysis

Data were analyzed using GraphPad Prism v7 (GraphPad Software Inc., USA) and are reported as mean ± S.E.M.. Statistical testing included *Student's* t-test, Mann-Whitney test or two-way ANOVA repeated measures, thereby considering data distribution and equality of variance. Specifically, to test for normal data distribution, Shapiro-Wilk's test was used, while the equality of variance was assessed using Levene's test. Differences between genotypes were considered to be significant when $p<0.05$.

3 Results

3.1 Autophagy-deprived cardiomyocytes show preserved Ca^{2+} handling at baseline

To investigate whether subcellular Ca^{2+} handling is altered in cardiomyocytes with defective autophagy under basal conditions, isolated cells were electrically stimulated at 1 Hz while being perfused with Tyrode's Solution containing 1 mmol/l $CaCl_2$ (representative recordings are shown below; Fig. 16A and 16B). At baseline, diastolic $[Ca^{2+}]_i$ of *Atg5*$^{+/+}$ *vs.* *Atg5*$^{-/-}$ cells were neither different in the cytoplasm (95.15 ± 8.96 nmol/l *vs.* 108.58 ± 14.44 nmol/l, p=0.418) nor the nucleus (189.52 ± 16.73 nmol/l *vs.* 226.70 ± 26.44 nmol/l, p=0.226). Furthermore, *Atg5*$^{+/+}$ and *Atg5*$^{-/-}$ cardiomyocytes displayed comparable cytoplasmic and nucleoplasmic Ca^{2+} transient peak amplitudes (553.02 ± 58.45 nmol/l and 261.25 ± 23.56 nmol/l *vs.* 679.90 ± 176.15 nmol/l and 316.40 ± 58.21 nmol/l, p=0.467 for the cytoplasm and p=0.355 for the nucleus). Also, there was neither a significant difference in the cytoplasmic and nucleoplasmic rise (TTP: 27 ± 2 ms and 189 ± 10 ms *vs.* 34 ± 3 ms and 191 ± 13 ms, p=0.076 for the cytoplasm and p=0.921 for the nucleus) nor half-decay time (DT_{50}: 161 ± 10 ms and 328 ± 11 ms *vs.* 173 ± 13 and 353 ± 12, p=0.466 for the cytoplasm and p=0.117 for the nucleus) in *Atg5*$^{+/+}$ *vs.* *Atg5*$^{-/-}$ cardiomyocytes (Fig. 16C).

Collectively, these findings demonstrate that the intracellular Ca^{2+} homeostasis of *Atg5*-deprived cardiomyocytes is preserved under basal conditions, suggesting that effective compensatory mechanisms prevent significant alterations of subcellular Ca^{2+} handling – at least under normal conditions – despite the loss of autophagy.

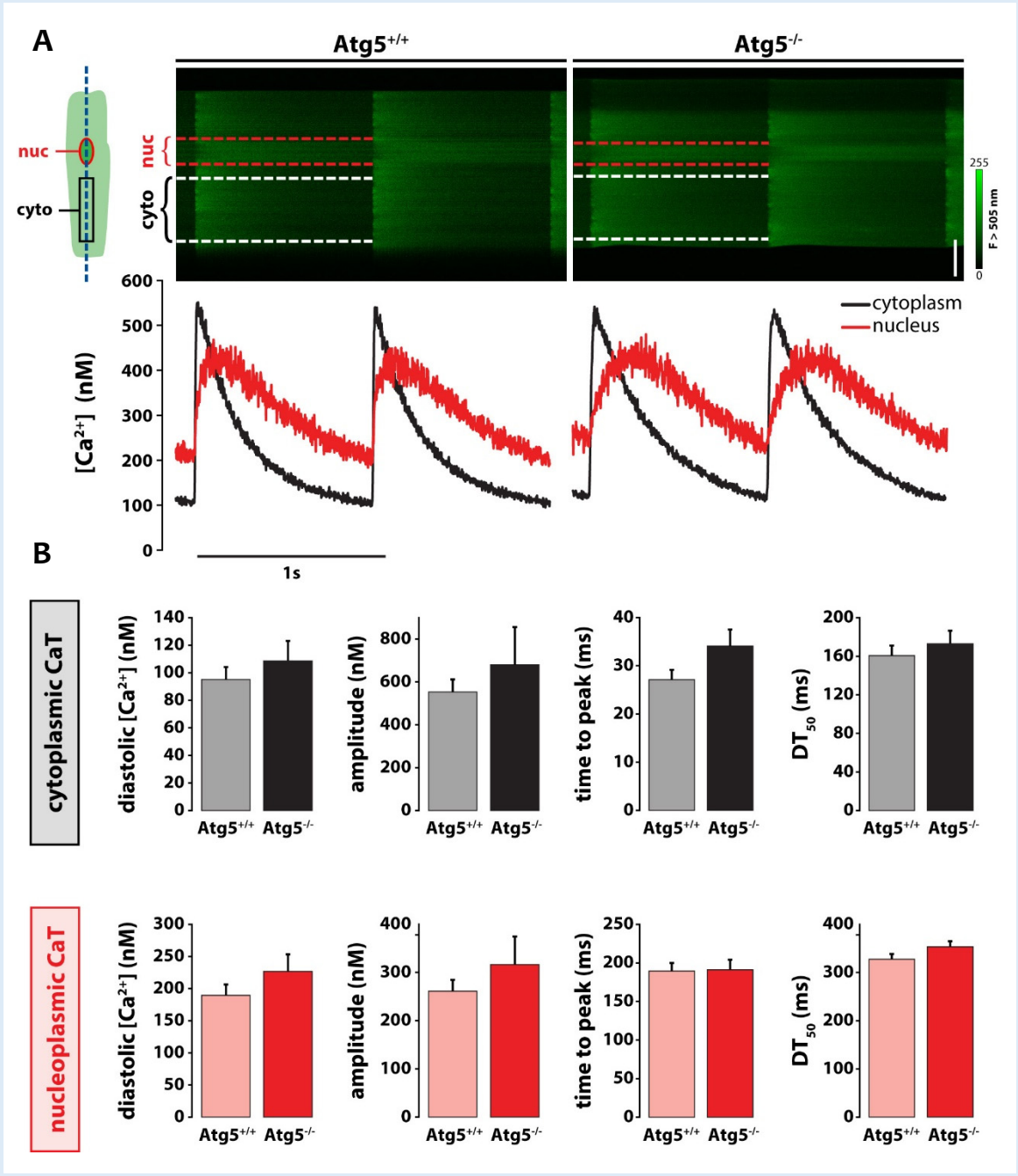

Figure 16: Characterization of Ca^{2+} transients of $Atg5^{+/+}$ vs. $Atg5^{-/-}$ cardiomyocytes under basal conditions. (A) Line-scan confocal microscopy was used to record Ca^{2+} transients in the cytoplasm (black rectangle) and nucleus (red circle), as indicated in the scheme on the left side. (B) Under basal conditions, main characteristics of cytoplasmic (black) and nucleoplasmic (red) Ca^{2+} transients were similar between groups. (C) At the basal state, diastolic $[Ca^{2+}]_i$, peak Ca^{2+} transient amplitudes, time-to-peak as well as DT_{50} of both cell compartments did not differ significantly, although *$Atg5^{-/-}$* cells tended to display increased diastolic $[Ca^{2+}]_i$ in both the cytoplasm as well as nucleus. For details see main text. n=20-24 cells from N=4-5 mice per group. Scale bar = 20 µm.

3.2 Autophagy-defective cells display preserved responsiveness of subcellular Ca^{2+} cycling to acute ß-adrenergic stress

Previously, it has been shown that *Atg5*-deprivation of cardiac myocytes enhances their susceptibility to adrenergic activation, leading to increased levels of apoptosis upon chronic ß-adrenergic stress (Nakai *et al.*, 2007). That said, we evaluated whether defective autophagy compromises subcellular Ca^{2+} homeostasis during ß-adrenergic stimulation. Acute isoprenaline administration expectedly increased Ca^{2+} transient amplitudes in the cytoplasm as well as the nucleus in both groups (representative recordings are shown below; Fig. 17). While diastolic $[Ca^{2+}]_i$ of cardiomyocytes lacking basal autophagy was significantly reduced upon ß-adrenergic stress in the cytoplasm as well as nucleus, this effect, however, was not observed in cardiomyocytes with intact autophagy. Furthermore, isoprenaline administration significantly increased Ca^{2+} transient's peak amplitudes in $Atg5^{+/+}$ and $Atg5^{-/-}$ cardiomyocytes in the cytoplasm (from 553.02 ± 58.45 to 989.47 ± 93.74 nmol/l, p<0.001 *vs.* from 679.90 ± 176.15 to 1098.80 ± 104.96 nmol/l, *p*=0.0045; respectively) as well as nucleus (from 261.25 ± 23.56 to 453.32 ± 39.58 nmol/l, p<0.0001 *vs.* from 316.40 ± 58.21 to 461.29 ± 44.57 nmol/l, *p*=0.0037; respectively), whereas we did not observe any significant differences between the two groups. While time-to-peak of the cytoplasmic Ca^{2+} transient was significantly increased upon ß-adrenergic stress in both

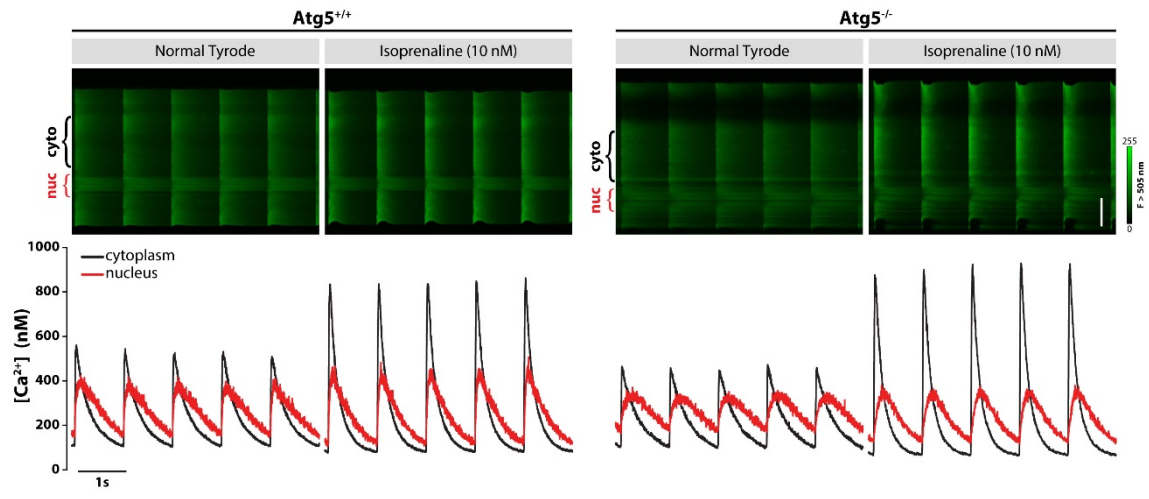

Figure 17: Representative Ca^{2+} traces at the basal state (Normal Tyrode, left panels) and during ß-adrenergic stress (Isoprenaline, right panels). Isoprenaline-administration increased Ca^{2+} amplitudes in the cytoplasm (black) as well as nucleus (red trace). The x-axis shows time. For details, see main text.

groups (*Atg5*$^{+/+}$: ? from 27 ± 2 to 30 ± 2 ms, *p*=0.021 *vs. Atg5*$^{-/-}$: ? from 34 ± 3 to 39 ± 3 ms, *p*=0.0043), there was a significant reduction of Ca^{2+} transient time-to-peak in the nucleus of *Atg5*$^{+/+}$ and *Atg5*$^{-/-}$ cells (from 189 ± 10 to 141 ± 13 ms, p<0.001 *vs.* from 191 ± 13 to 147 ± 9 ms, *p*=0.0012, respectively), likely due to the delayed kinetics and smaller amplitudes of nucleoplasmic Ca^{2+} transients. Moreover, ß-adrenergic activation resulted in shortened half-decay time in the cytoplasm (from 161 ± 10 to 110 ± 6 ms, p<0.001 *vs.*from 173 ± 13 to 110 ± 6 ms, p<0.001) as well as nucleus (from 328 ± 11 to 270 ± 13 ms, p<0.001 *vs.* from 353 ± 12 to 277 ± 11 ms, p<0.001) in both *Atg5*$^{+/+}$ and *Atg5*$^{-/-}$ cells, respectively (Fig. 18). SR Ca^{2+} load was assessed by high-dose caffeine administration upon isoprenaline exposure. Thereby, high-dose caffeine application increased fluorescence intensity to the same extent in both groups (F/F_0: 10.1 ±0 .6 *vs.* 9.3 ± 0.3 in *Atg5*$^{+/+}$ and *Atg5*$^{-/-}$ cells, respectively).

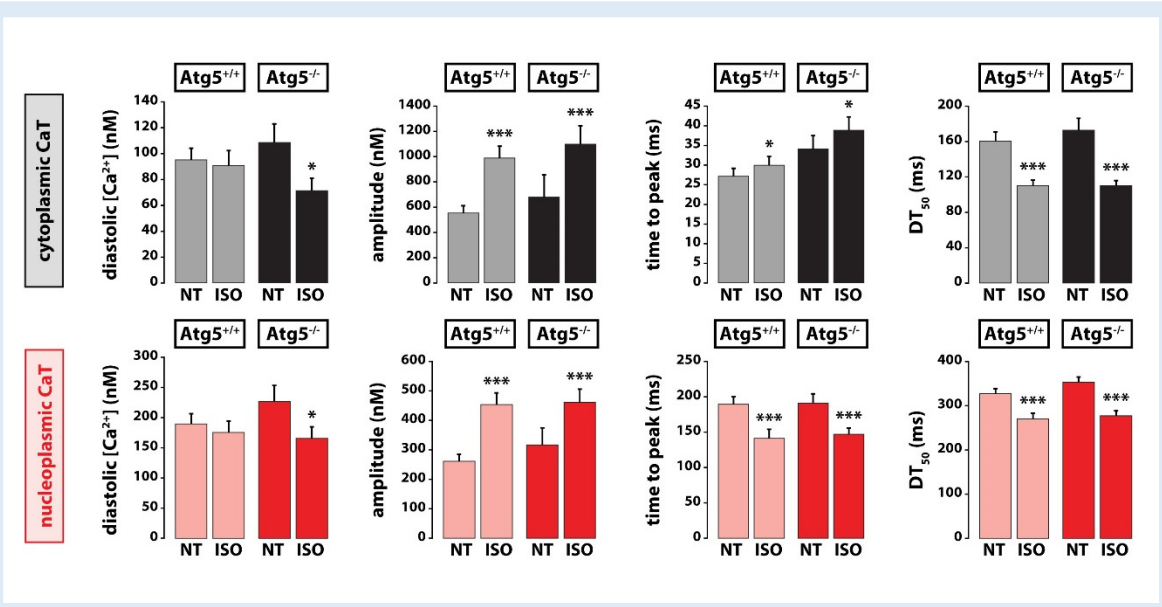

Figure 18: Effect of ß-adrenergic stimulation on cytoplasmic (upper panels) and nucleoplasmic (lower panels) Ca^{2+} homeostasis in Atg5$^{+/+}$ vs. Atg5$^{-/-}$ cells. While diastolic $[Ca^{2+}]_i$ was not significantly altered upon ß-adrenergic stress in *Atg5*$^{+/+}$ cells, ß-adrenergic activation induced a significant reduction of the diastolic $[Ca^{2+}]_i$ in cardiomyocytes with defective autophagy. ß-adrenergic response on intracellular Ca^{2+} handling also lead to a significant increase in Ca^{2+} transient peak amplitudes and reduction of half-decay time (DT_{50}) in the cytoplasm as well as nucleus. While we observed a significant increase in time-to-peak of the cytoplasmic Ca^{2+} transients upon ß-adrenergic stimulation, there was an increase in the time-to-peak of nucleoplasmic Ca2+ transients. Abbreviations: NT, Normal Tyrode; ISO, Isoprenaline. n=22-24 cardiomyocytes from N=4-5 mice per group. Scale bar = 20 µm. *P<0.05 ***P<0.001

3.3 Frequency-dependent Ca^{2+} cycling is altered in autophagy-deprived cardiomyocytes

Besides the effects on contractility (i.e. positive inotropy), systemic circulating β-adrenergic agonists (e.g. isoprenaline) also increase the contraction frequency of the myocardium (i.e. positive chronotropy). To assess, whether subcellular Ca^{2+} homeostasis is altered during such conditions of high ATP demand, cardiomyocytes were stimulated at different pacing frequencies, namely 1, 2, 3 and 4 Hz. Thereby, increasing pacing frequencies resulted in enhanced diastolic $[Ca^{2+}]_i$ in the cytoplasm as well as nucleus in both groups (representative Ca^{2+} transients are shown below in Figure 19). However, while we observed a significant frequency-dependent increase in Ca^{2+} transient peak amplitudes in *Atg5*$^{+/+}$ cells, this positive relationship was blunted in *Atg5*$^{-/-}$ cardiomyocytes, both in the cytoplasm (2 Hz: 307.35 ± 35.14 *vs.* 220.52 ± 18.74 nmol/l, *p*=0.026; 3 Hz: 392.60 ± 50.36 *vs.* 277.27 ± 27.44 nmol/l, *p*=0.039; 4 Hz: 403.14 ± 62.58 *vs.* 258.02 ± 28.49 nmol/l, *p*=0.031) as well as nucleus (2 Hz: 126.14 ± 11.74 *vs.* 95.63 ± 9.17 nmol/l, *p*=0.044; 3 Hz: 169.89 ± 26.56 *vs.* 111.15 ± 13.88 nmol/l, *p*=0.0044; 4 Hz: 185.77 ± 28.48 *vs.* 107.08 ±

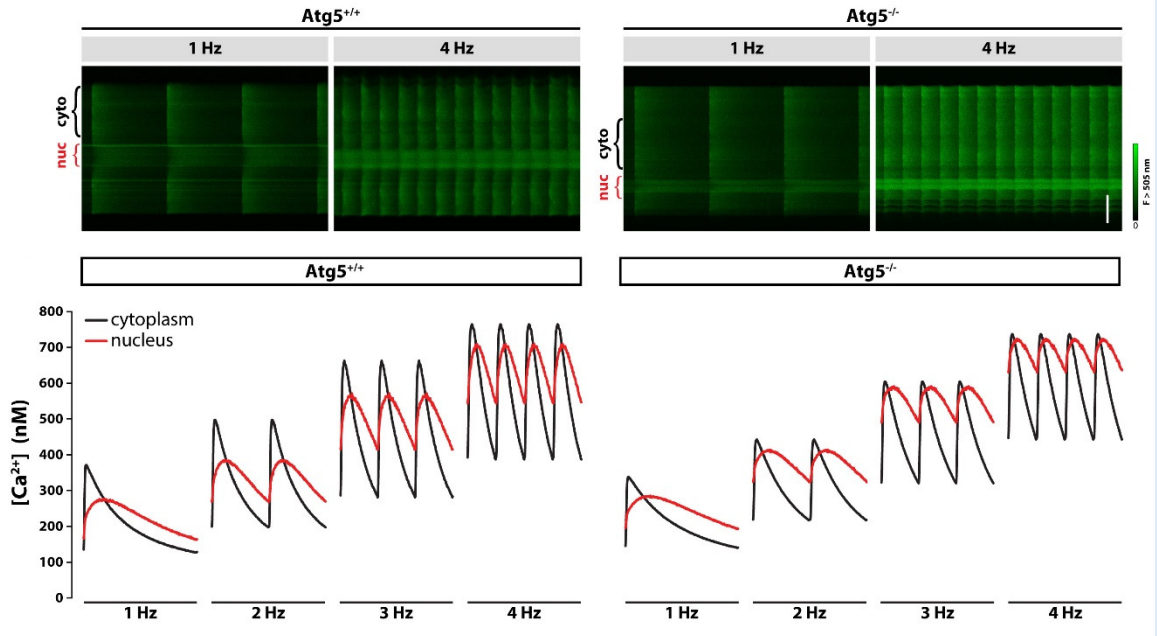

Figure 19: Characterization of cytoplasmic and nucleoplasmic Ca^{2+} transients in Atg5$^{+/+}$ vs. Atg5$^{-/-}$ cells paced at different stimulation frequencies. The upper panels show representative line-scan imaging of Ca^{2+} transients obtained from cardiomyocytes paced at 1 and 4 Hz. Diastolic $[Ca^{2+}]_i$ expectedly increased upon high-frequency stimulation in *Atg5*$^{+/+}$ and *Atg5*$^{-/-}$ cardiomyocytes, as illustrated in the lower panels.

12.40 nmol/l M, *p*=0.010; Fig. 21 A). Based on the delayed kinetics of nucleoplasmic Ca^{2+} transients, higher stimulation frequencies typically result in an augmented $[Ca^{2+}]_i$ during diastole (Ljubojević *et al.*, 2011). During conditions of compromised SERCA2a activity (e.g. owing to ATP depletion or downregulated protein expression), the dysproportional build-up of diastolic $[Ca^{2+}]_i$ may subsequently lead to enhanced nucleoplasmic Ca^{2+} load (Ljubojevic *et al.*, 2014). Indeed, the frequency-dependent increase in nucleoplasmic Ca^{2+} load was more pronounced in *Atg5*-deprived cardiomyocytes, suggesting reduced SERCA2a function during conditions of high ATP demand, and may therefore be critically involved in Ca^{2+} mediated transcriptional regulation (*Atg5*$^{+/+}$ *vs. Atg5*$^{-/-}$ cardiomyocytes, 1 Hz: 44.95 ± 7.63 *vs.* 52.88 ± 9.08 nMs^{-1}, 2 Hz: 66.71 ± 5.51 *vs.* 81.66 ± 7.10 nMs^{-1}, 3 Hz: 96.53 ± 8.37 *vs.* 118.49 ± 7.61 nMs^{-1}, 4 Hz: 126.34 ± 7.22 *vs.* 147.63 ± 7.51 nMs^{-1}; p<0.05, Fig. 21 B).

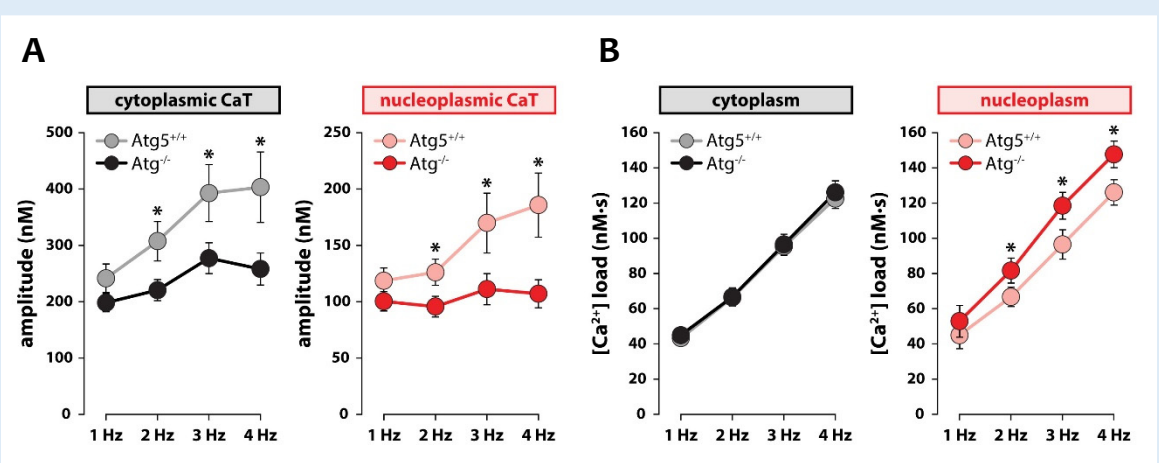

Figure 20: Frequency-dependent alterations of Ca^{2+} transient amplitudes (left panels) and intracellular Ca^{2+} load (right panels). (A) While cytoplasmic and nucleoplasmic Ca^{2+} transient amplitudes significantly increased in cardiomyocytes with intact autophagy, this effect was not seen in cardiomyocytes with inhibited autophagy. (B) Higher stimulation frequencies induced a similar increase in cytoplasmic Ca^{2+} load in both groups. However, the increase in nucleoplasmic Ca^{2+} load was more pronounced in *Atg5*$^{-/-}$ cells, when compared to the control group. n=19-25 cells from N=3 mice per group. *P<0.05

4 Discussion

The present study provides compelling evidence that autophagy is critically involved in the maintenance of subcellular Ca^{2+} homeostasis of left ventricular cardiomyocytes paced at high stimulation frequencies. Deprivation of this housekeeping mechanism (i.e. autophagy) results in alterations of cytoplasmic and nucleoplasmic Ca^{2+} handling early in life, which may be causaly involved in hypertrophic gene program activation.

During ECC, membrane depolarization and subsequent activation of L-type Ca^{2+} channels allow extracellular Ca^{2+} to enter the cytoplasmic compartment. In doing so, the binding of intracellular Ca^{2+} to the RyR2 induces the bulk of Ca^{2+} to be released from the SR, which in turn enables Ca^{2+} to bind troponin C and, thus, to initiate conformational changes resulting in myocardial contraction. For relaxation to occur, the ATP-dependent reuptake of Ca^{2+} by SERCA2a and sarcolemmal Ca^{2+} extrusion by NCX play a key role in both, human and mouse hearts. Thereby, contractile force is not only modulated by length-dependent stretch (i.e. Frank-Starling mechanism) or frequency-dependent activation (i.e. Bowditch effect), but also by the autonomic nervous system (e.g. ß-adrenergic stimulation). Both, PLB (mainly leading to accelerated Ca^{2+} uptake by SERCA2a) and TnI phosphorylation (resulting in altered myofilament Ca^{2+} sensitivity) by ß-adrenergic activation enhance the rate of myocardial relaxation and are, therefore, key elements during conditions of increased workload (Karczewski *et al.*, 1990).

Our findings indicate that dysfunctional autophagy does not alter Ca^{2+} transient peak amplitudes and kinetics (i.e. TTP and DT_{50}) at baseline neither in the cytoplasm nor in the nucleus. Contrary, however, *Atg5*-deprived cardiomyocytes displayed severe alterations of subcellular Ca^{2+} handling, when paced at higher frequencies (2-4 Hz), underlining their high vulnerability to stress. Thereby, *Atg5*$^{-/-}$ cells lacked the ability to increase their cytoplasmic and nucleoplasmic Ca^{2+} transient peak amplitudes to an appropriate level upon gradual exposure to increasing pacing frequencies. To assess, whether the stress-induced alterations of subcellular Ca^{2+} handling are caused by compromised activity states of PLB or TnI, extracted hearts were retrogradely perfused with isoprenaline (10 nmol/l) for 5 minutes and subjected to Western Blot analysis. Intriguingly, while the phosphorylation and, thus, activation of PLB was fully intact, the phosphorylation of TnI was compromised

in *Atg5*-deprived hearts exposed to isoprenaline (our unpublished data). In contrast, however, we did not observe any differences in SERCA2a levels and activation under normal conditions and during ß-adrenergic stress. The predominance of PLB phosphorylation over TnI as well as preserved SERCA2a activation and protein levels at baseline and upon ß-adrenergic stress suggest that shortage of intracellular ATP may be the main cause for the disturbances of subcellular Ca^{2+} homeostasis in autophagy-defective hearts.

By increasing the beat frequency and the stroke volume, the heart can rapidly adapt cardiac output to match continuously changing physiological demands of the body. To do so, high levels of intracellular ATP are necessary to allow subcellular Ca^{2+} cycling to adapt appropriately. Thereby, the Ca^{2+}-dependent myofilament ATPase and other ATPases involved in ion flux, such as SERCA2a, consume the bulk of ATP available (Bers, 2008). In wild-type mice, the ß-adrenergic agonist isoproterenol has been shown to reduce myofilament sensitivity to Ca^{2+} and to cause an increase of the peak ATPase rate, whereas these effects were abolished in transgenic mice expressing TnI incapable of being phosphorylated on serines$^{23/24}$ (Pi *et al.*, 2003). TnI phosphorylation by PKA may, therefore, require high levels of both intracellular Ca^{2+} and ATP, and its reduced phosphorylation may be a compensatory mechanism promoting efficient ATP utilization during increased workload. The lack of intracellular ATP due to aberrant structural and functional changes of mitochondria (Taneike *et al.*, 2010) may well contribute to subcellular alterations of cardiac Ca^{2+} homeostasis, and reduced phosphorylation of TnI which precede cardiac dysfunction, possibly playing a causative role in the development and acceleration of hypertrophic remodeling processes observed in the *Atg5*-deficient genotype.

Besides its central involvement in regulating the contractility of the beating heart, subcellular Ca^{2+} acts as a key signal shaping cardiac gene programming. At higher frequencies, nucleoplasmic Ca^{2+} transients tend to display higher diastolic $[Ca^{2+}]_i$ due to the passive and, thus, delayed diffusion of Ca^{2+} through NPC. In the nucleus of mice lacking *Atg5*, however, the frequency-dependent disproportional build-up of diastolic $[Ca^{2+}]_i$ suggests impaired SERCA2a function and may, therefore, be critically involved in Ca^{2+}-mediated hypertrophic gene signaling. The CaMKII-HDAC and CaN-NFAT pathways are considered two major Ca^{2+}-CaM-dependent pathways implicated in hypertrophic gene

program activation. CaN features a much higher Ca^{2+}-CaM affinity as compared to CaMKII, and, as such, may be superior in sensing lower levels of sustained elevations in $[Ca^{2+}]_i$, similar to those observed in *Atg5*-deprived myocytes at high stimulation frequencies. Hence, we hypothesize that early perturbations of subcellular Ca^{2+} handling may be a critical determinant in the development and progression of cardiac remodeling in mice with defective autophagy. In support of this hypothesis, we observed attenuated *Atg5* protein levels in both compensated hypertrophy and failing human hearts, and, most importantly, found a significant inverse correlation between *Atg5* protein expression and the extent of hypertrophic remodeling in human hearts (our unpublished data).

To our knowledge, this study demonstrates – for the first time – that frequency-dependent subcellular Ca^{2+} cycling is significantly altered in cardiomyocytes with defective autophagy early in life. Given the early onset of disturbances of subcellular Ca^{2+} handling, these changes may be critically involved in hypertrophic gene program activation. Further research is warranted to directly (dis)prove whether this observation is caused by a mismatch of ATP supply and demand in cardiomyocytes upon acute or chronic stress.

5 References

Abdellatif, M. *et al.* (2018) 'Autophagy in Cardiovascular Aging', *Circulation research*, 123(7), pp. 803–824. doi: 10.1161/CIRCRESAHA.118.312208.

Anderson, M. E. (2012) 'Connections Count', *Circulation Research*, 86(7), pp. 717–719. doi: 10.1161/01.res.86.7.717.

Andersson, C. *et al.* (2010) 'Metformin treatment is associated with a low risk of mortality in diabetic patients with heart failure: A retrospective nationwide cohort study', *Diabetologia*, 53(12), pp. 2546–2553. doi: 10.1007/s00125-010-1906-6.

Atar, D. *et al.* (1995) 'Excitation-transcription coupling mediated by zinc influx through voltage-dependent calcium channels', *Journal of Biological Chemistry*, 270(6), pp. 2473–2477. doi: 10.1074/jbc.270.6.2473.

Awad, S. *et al.* (2013) 'Nuclear CaMKII enhances histone H3 phosphorylation and remodels chromatin during cardiac hypertrophy', *Nucleic Acids Research*, 41(16), pp. 7656–7672. doi: 10.1093/nar/gkt500.

Baddeley, D. *et al.* (2009) 'Optical single-channel resolution imaging of the ryanodine receptor distribution in rat cardiac myocytes', *Proceedings of the National Academy of Sciences*, 106(52), pp. 22275–22280. doi: 10.1073/pnas.0908971106.

Bassani, J. W., Bassani, R. A. and Bers, D. M. (1994) 'Relaxation in rabbit and rat cardiac cells: species-dependent differences in cellular mechanisms.', *The Journal of Physiology*, 476(2), pp. 279–293. doi: 10.1113/jphysiol.1994.sp020130.

Bassani, J. W., Yuan, W. and Bers, D. M. (1995) 'Fractional SR Ca release is regulated by trigger Ca and SR Ca content in cardiac myocytes.', *The American journal of physiology*, 268(5 Pt 1), pp. C1313-9. doi: 10.1152/ajpcell.1995.268.5.C1313.

Bergmann, O. *et al.* (2009) 'Evidence for cardiomyocyte renewal in humans', *Science*, 324(5923), pp. 98–102. doi: 10.1126/science.1164680.

Bers, D. M. (2001) *Excitation-Contraction Coupling and Cardiac Contractile Force*. doi: 10.1093/cvr/26.4.430.

Bers, D. M. (2002) 'Cardiac excitation–contraction coupling', *Nature*, 415(6868), pp. 198–205. doi: 10.1038/415198a.

Bers, D. M. (2008) 'Calcium Cycling and Signaling in Cardiac Myocytes', *Annual Review of Physiology*, 70(1), pp. 23–49. doi: 10.1146/annurev.physiol.70.113006.100455.

Bers, D. M. (2011) 'Ca2+-calmodulin-dependent protein kinase II regulation of cardiac excitation-transcription coupling', *Heart Rhythm*. Elsevier Inc., 8(7), pp. 1101–1104. doi: 10.1016/j.hrthm.2011.01.030.

Bers, D. M. and Guo, T. (2005) 'Calcium signaling in cardiac ventricular myocytes', *Annals of the New York Academy of Sciences*, 1047, pp. 86–98. doi: 10.1196/annals.1341.008.

Bootman, M. D. *et al.* (2013) 'Ca2+-sensitive fluorescent dyes and intracellular Ca2+ imaging', *Cold Spring Harbor Protocols*, 8(2), pp. 83–99. doi: 10.1101/pdb.top066050.

Boudina, S. and Abel, E. D. (2010) 'Diabetic cardiomyopathy, causes and effects.', *Rev Endocr Metab Disord*, 11(1), pp. 31--39. doi: 10.1007/s11154-010-9131-7.

Bravo-San Pedro, J. M., Kroemer, G. and Galluzzi, L. (2017) 'Autophagy and Mitophagy in Cardiovascular Disease', *Circulation Research*, pp. 1812–1824. doi: 10.1161/CIRCRESAHA.117.311082.

Brittsan, A. G. and Kranias, E. G. (2000) 'Phospholamban and cardiac contractile function', *Journal of Molecular and Cellular Cardiology*, 32(12), pp. 2131–2139. doi: 10.1006/jmcc.2000.1270.

Bround, M. J. *et al.* (2013) 'Cardiomyocyte ATP production, metabolic flexibility, and survival require calcium flux through cardiac ryanodine receptors in vivo', *Journal of Biological Chemistry*, 288(26), pp. 18975–18986. doi: 10.1074/jbc.M112.427062.

Bueno, O. F. *et al.* (2002) 'Calcineurin and hypertrophic heart disease: Novel insights and remaining questions', *Cardiovascular Research*, 53(4), pp. 806–821. doi: 10.1016/S0008-6363(01)00493-X.

Burkard, N. *et al.* (2005) 'Targeted proteolysis sustains calcineurin activation', *Circulation*, 111(8), pp. 1045–1053. doi: 10.1161/01.CIR.0000156458.80515.F7.

Cantó, C. *et al.* (2009) 'AMPK regulates energy expenditure by modulating NAD + metabolism and SIRT1 activity', *Nature*, 458(7241), pp. 1056–1060. doi: 10.1038/nature07813.

Choi, A. M. K., Ryter, S. W. and Levine, B. (2013) 'Autophagy in Human Health and Disease', *New England Journal of Medicine*, 368(7), pp. 651–662. doi: 10.1056/NEJMra1205406.

Cuervo, A. M. *et al.* (2005) 'Autophagy and aging: the importance of maintaining "clean" cells.', *Autophagy*, 1(3), pp. 131–140. doi: 10.4161/auto.1.3.2017.

Dewenter, M. *et al.* (2017) 'Calcium signaling and transcriptional regulation in cardiomyocytes', *Circulation Research*, 121(8), pp. 1000–1020. doi: 10.1161/CIRCRESAHA.117.310355.

Donati, A. *et al.* (2001) 'Age-related changes in the regulation of autophagic proteolysis in rat isolated hepatocytes', *Journals of Gerontology - Series A Biological Sciences and Medical Sciences*, 56(7), pp. B288–B293. doi: 10.1093/gerona/56.7.B288.

Eisenberg, T. *et al.* (2016) 'Cardioprotection and lifespan extension by the natural polyamine spermidine', *Nature Medicine*, 22(12), pp. 1428–1438. doi: 10.1038/nm.4222.

Eisner, D. A. *et al.* (2017) 'Calcium and Excitation-Contraction Coupling in the Heart', *Circulation Research*, 121(2), pp. 181–195. doi: 10.1161/CIRCRESAHA.117.310230.

Endo, Y., Furuta, A. and Nishino, I. (2015) 'Danon disease: a phenotypic expression of LAMP-2 deficiency', *Acta Neuropathologica*, pp. 391–398. doi: 10.1007/s00401-015-1385-4.

Endoh, M. and Blinks, J. R. (1988) 'Actions of sympathomimetic amines on the Ca2+ transients and contractions of rabbit myocardium: reciprocal changes in myofibrillar responsiveness to Ca2+ mediated through alpha- and beta-adrenoceptors', *Circulation Research*, 62, pp. 247–265. Available at: https://doi.org/10.1161/01.RES.62.2.247.

Fabiato, A. (1983) 'Calcium-induced release of calcium from the cardiac sarcoplasmic reticulum', *American Journal of Physiology-Cell Physiology*, 245(1), pp. C1–C14. doi: 10.1152/ajpcell.1983.245.1.c1.

Ferrari, A. U., Radaelli, A. and Centola, M. (2003) 'Invited Review: Aging and the cardiovascular system', *Journal of Applied Physiology*, 95(6), pp. 2591–2597. doi: 10.1152/japplphysiol.00601.2003.

Finkler, A., Ashery-Padan, R. and Fromm, H. (2007) 'CAMTAs: Calmodulin-binding transcription activators from plants to human', *FEBS Letters*. Federation of European Biochemical Societies, 581(21), pp. 3893–3898. doi: 10.1016/j.febslet.2007.07.051.

Frey, N., McKinsey, T. A. and Olson, E. N. (2000) 'Decoding calcium signals involved in cardiac growth and function', *Nature Medicine*, 6(11), pp. 1221–1227. doi: 10.1038/81321.

Galluzzi, L. *et al.* (2014) 'Metabolic control of autophagy', *Cell*. Elsevier Inc., 159(6), pp. 1263–1276. doi: 10.1016/j.cell.2014.11.006.

Ge, L. *et al.* (2017) 'Remodeling of ER-exit sites initiates a membrane supply pathway for autophagosome biogenesis', *EMBO reports*, 18(9), pp. 1586–1603. doi: 10.15252/embr.201744559.

Gee, K. R. *et al.* (2000) 'Chemical and physiological characterization of fluo-4 Ca2+-indicator dyes', *Cell Calcium*, 27(2), pp. 97–106. doi: 10.1054/ceca.1999.0095.

Gray CB, Suetomi T, Xiang S, Mishra S, Blackwood EA, Glembotski CC, Miyamoto S, Westenbrink BD, B. J. (2017) 'CaMKIIδ subtypes differentially regulate infarct formation following ex vivo myocardial ischemia/reperfusion through NF-κB and TNF-α', p. J Mol Cell Cardiol. doi: 10.1016/j.yjmcc.2017.01.002.

Gundewar, S. *et al.* (2009) 'Activation of AMP-activated protein kinase by metformin improves left ventricular

function and survival in heart failure', *Circulation Research*, 104(3), pp. 403–411. doi: 10.1161/CIRCRESAHA.108.190918.

Gurusamy, N. *et al.* (2009) 'Cardioprotection by adaptation to ischaemia augments autophagy in association with BAG-1 protein', *Journal of Cellular and Molecular Medicine*, 13(2), pp. 373–387. doi: 10.1111/j.1582-4934.2008.00495.x.

Gustafsson, Å. B. and Gottlieb, R. A. (2009) 'Autophagy in ischemic heart disease', *Circulation Research*, 104(2), pp. 150–158. doi: 10.1161/CIRCRESAHA.108.187427.

Haigis, M. C. and Sinclair, D. A. (2010) 'Mammalian Sirtuins: Biological Insights and Disease Relevance', *Annual Review of Pathology: Mechanisms of Disease*, 5(1), pp. 253–295. doi: 10.1146/annurev.pathol.4.110807.092250.

Hailey, D. W. *et al.* (2010) 'Mitochondria Supply Membranes for Autophagosome Biogenesis during Starvation', *Cell*. Elsevier Ltd, 141(4), pp. 656–667. doi: 10.1016/j.cell.2010.04.009.

Hallhuber, M. *et al.* (2006) 'Inhibition of nuclear import of calcineurin prevents myocardial hypertrophy', *Circulation Research*, 99(6), pp. 626–635. doi: 10.1161/01.RES.0000243208.59795.d8.

Haq, S. *et al.* (2001) 'Human Hearts With Hypertrophy Versus Advanced', *Heart Failure*, pp. 670–677.

Hariharan, N. *et al.* (2010) 'Deacetylation of FoxO by Sirt1 plays an essential role in mediating starvation-induced autophagy in cardiac myocytes', *Circulation Research*, 107(12), pp. 1470–1482. doi: 10.1161/CIRCRESAHA.110.227371.

Hasenfuss, G. and Pieske, B. (2002) 'Calcium cycling in congestive heart failure', *Journal of Molecular and Cellular Cardiology*, 34(8), pp. 951–969. doi: 10.1006/jmcc.2002.2037.

He, C. *et al.* (2013) 'Dissociation of Bcl-2-Beclin1 complex by activated AMPK enhances cardiac autophagy and protects against cardiomyocyte apoptosis in diabetes', *Diabetes*, 62(4), pp. 1270–1281. doi: 10.2337/db12-0533.

Hill, J. A. and Olson, E. N. (2008) 'Cardiac Plasticity', *New England Journal of Medicine*, 358(13), pp. 1370–1380. doi: 10.1056/NEJMra072139.

Horiuchi-Hirose, M. *et al.* (2010) ' Decrease in the density of t-tubular L-type Ca 2+ channel currents in failing ventricular myocytes ', *American Journal of Physiology-Heart and Circulatory Physiology*, 300(3), pp. H978–H988. doi: 10.1152/ajpheart.00508.2010.

Johnson, S. C., Rabinovitch, P. S. and Kaeberlein, M. (2013) 'MTOR is a key modulator of ageing and age-related disease', *Nature*, 493(7432), pp. 338–345. doi: 10.1038/nature11861.

Karczewski, P., Bartel, S. and Krause, E. G. (1990) 'Differential sensitivity to isoprenaline of troponin I and phospholamban phosphorylation in isolated rat hearts', *Biochemical Journal*, 266(1), pp. 115–122. doi: 10.1042/bj2660115.

Kirchhefer, U. *et al.* (1999) 'Activity of cAMP-dependent protein kinase and Ca2+/calmodulin- dependent protein kinase in failing and nonfailing human hearts', *Cardiovascular Research*, 42(1), pp. 254–261. doi: 10.1016/S0008-6363(98)00296-X.

Kockskamper, J. *et al.* (2007) 'Endothelin-1 enhances nuclear Ca2+ transients in atrial myocytes through Ins(1,4,5)P3-dependent Ca2+ release from perinuclear Ca2+ stores', *Journal of Cell Science*, 121(2), pp. 186–195. doi: 10.1242/jcs.021386.

Kohl, T. *et al.* (2013) 'Superresolution microscopy in heart - Cardiac nanoscopy', *Journal of Molecular and Cellular Cardiology*. Elsevier Ltd, 58(1), pp. 13–21. doi: 10.1016/j.yjmcc.2012.11.016.

Kroemer, G., Mariño, G. and Levine, B. (2010) 'Autophagy and the Integrated Stress Response', *Molecular Cell*, 40(2), pp. 280–293. doi: 10.1016/j.molcel.2010.09.023.

Lehmann, L. H. *et al.* (2014) 'Histone deacetylase signaling in cardioprotection', *Cellular and Molecular Life Sciences*, 71(9), pp. 1673–1690. doi: 10.1007/s00018-013-1516-9.

Lehnart, S. E., Maier, L. S. and Hasenfuss, G. (2009) 'Abnormalities of calcium metabolism and myocardial contractility depression in the failing heart', *Heart Failure Reviews*, 14(4), pp. 213–224. doi: 10.1007/s10741-009-9146-x.

Lim, H. W. and Molkentin, J. D. (1999) 'Calcineurin and human heart failure [1]', *Nature Medicine*, 5(3), pp. 246–247. doi: 10.1038/6430.

Ljubojevic, S. *et al.* (2014) 'Early remodeling of perinuclear Ca2+ stores and nucleoplasmic Ca2+ signaling during the development of hypertrophy and heart failure', *Circulation*, 130(3), pp. 244–255. doi: 10.1161/CIRCULATIONAHA.114.008927.

Ljubojević, S. *et al.* (2011) 'In situ calibration of nucleoplasmic versus cytoplasmic Ca2+ concentration in adult cardiomyocytes', *Biophysical Journal*, 100(10), pp. 2356–2366. doi: 10.1016/j.bpj.2011.03.060.

Ljubojevic, S. and Bers, D. M. (2015) 'Nuclear calcium in cardiac myocytes', *Journal of Cardiovascular Pharmacology*, 65(3), pp. 211–217. doi: 10.1097/FJC.0000000000000174.

Louch, W. E., Sheehan, K. A. and Wolska, B. M. (2011) 'Methods in Cardiomyocyte Isolation, Culture, and Gene Transfer', *J Mol Cell Cardiol.*, 51(3), pp. 288–298. doi: 10.1016/j.yjmcc.2011.06.012.Methods.

Luo, M. and Anderson, M. E. (2013) 'Mechanisms of altered Ca2+ handling in heart failure', *Circulation Research*, 113(6), pp. 690–708. doi: 10.1161/CIRCRESAHA.113.301651.

Marks, A. R. (2013) 'Calcium cycling proteins and heart failure: Mechanisms and therapeutics', *Journal of Clinical Investigation*, 123(1), pp. 46–52. doi: 10.1172/JCI62834.

Matsui, Y. *et al.* (2007) 'Distinct roles of autophagy in the heart during ischemia and reperfusion: Roles of AMP-activated protein kinase and beclin 1 in mediating autophagy', *Circulation Research*, 100(6), pp. 914–922. doi: 10.1161/01.RES.0000261924.76669.36.

Mauger, J. P. (2012) 'Role of the nuclear envelope in calcium signalling', *Biology of the Cell*, 104(2), pp. 70–83. doi: 10.1111/boc.201100103.

McNutt, N. S. (1969) 'The Ultrastructure of the Cat Myocardium: I. Ventricular Papillary Muscle', *The Journal of Cell Biology*, 42(1), pp. 46–67. doi: 10.1083/jcb.42.1.46.

De Meyer, G. R. Y., De Keulenaer, G. W. and Martinet, W. (2010) 'Role of autophagy in heart failure associated with aging', *Heart Failure Reviews*, 15(5), pp. 423–430. doi: 10.1007/s10741-010-9166-6.

Molkentin, J. D. (2000) 'Calcineurin and Beyond - Cardiac Hypertrophic Signaling', *Circulation Research*, 87, pp. 731–738.

Morozova, K. *et al.* (2015) 'Annexin A2 promotes phagophore assembly by enhancing Atg16L+ vesicle biogenesis and homotypic fusion', *Nature Communications*. doi: 10.1038/ncomms6856.

Mukhopadhyay, S. *et al.* (2015) 'Reciprocal regulation of AMP-activated protein kinase and phospholipase D', *Journal of Biological Chemistry*, 290(11), pp. 6986–6993. doi: 10.1074/jbc.M114.622571.

Nair, S. and Ren, J. (2012) 'Autophagy and cardiovascular aging: Lesson learned from rapamycin', *Cell Cycle*, 11(11), pp. 2092–2099. doi: 10.4161/cc.20317.

Nakai, A. *et al.* (2007) 'The role of autophagy in cardiomyocytes in the basal state and in response to hemodynamic stress', *Nature Medicine*, 13(5), pp. 619–624. doi: 10.1038/nm1574.

Nishida, K. *et al.* (2009) 'The role of autophagy in the heart', *Cell Death and Differentiation*, 16(1), pp. 31–38. doi: 10.1038/cdd.2008.163.

Nishino, I. *et al.* (2000) 'Primary LAMP-2 deficiency causes X-linked vacuolar cardiomyopathy and\nmyopathy (Danon disease)', *Nature*, 406(6798), pp. 906–910. doi: 10.1038/35022604.

O'Connell, T. D. *et al.* (2003) 'Isolation and Culture of Adult Mouse Cardiac Myocytes for Signaling Studies', *AfCS Research Reports*, 1(5), pp. 1–9. doi: 10.1385/1-59745-214-9:271.

O'Connell, T. D., Rodrigo, M. C. and Simpson, P. C. (2007) 'Isolation and culture of adult mouse cardiac

myocytes.', *Methods in molecular biology (Clifton, N.J.)*, 357(7), pp. 271–96. doi: 10.1385/1-59745-214-9:271.

Orogo, A. M. and Gustafsson, ??sa B. (2015) 'Therapeutic targeting of autophagy potential and concerns in treating cardiovascular disease', *Circulation Research*. doi: 10.1161/CIRCRESAHA.116.303791.

Pedrozo, Z. *et al.* (2013) 'Cardiomyocyte ryanodine receptor degradation by chaperone-mediated autophagy', *Cardiovascular Research*, 98(2), pp. 277–285. doi: 10.1093/cvr/cvt029.

Peterson, B. Z. *et al.* (1999) 'Erratum: Calmodulin is the Ca2+ sensor for Ca2+-dependent inactivation of L-type calcium channels (Neuron (March 1999))', *Neuron*, 22(4), p. 844. doi: 10.1016/S0896-6273(00)80742-4.

Pi, Y. Q. *et al.* (2003) 'Protein kinase C and A sites on troponin I regulate myofilament Ca2+ sensitivity and ATPase activity in the mouse myocardium', *Journal of Physiology*, 552(3), pp. 845–857. doi: 10.1113/jphysiol.2003.045260.

Porrello, E. R. *et al.* (2009) 'Angiotensin II type 2 receptor antagonizes angiotensin ii type 1 receptor-mediated cardiomyocyte autophagy', *Hypertension*, 53(6), pp. 1032–1040. doi: 10.1161/HYPERTENSIONAHA.108.128488.

Puglisi, J. L. *et al.* (1999) 'Ca2+ Influx Through Ca2+ Channels in Rabbit Ventricular Myocytes During Action Potential Clamp : Influence of Temperature', *Circulation Research*, 85(6), pp. e7–e16. doi: 10.1161/01.RES.85.6.e7.

Reuter, H. *et al.* (1999) 'Calmodulin supports both inactivation and facilitation of L-type calcium channels.', *Nature*, 399(6732), pp. 159–162. doi: 10.1038/20200.

Ringer, S. (1883) 'A further Contribution regarding the influence of the different Constituents of the Blood on the Contraction of the Heart', *American Journal of Physiology*, 245, pp. C1–C14. doi: 10.1113/jphysiol.1883.sp000120.

Rothermel, B. A. and Hill, J. A. (2007) 'Erratum: Myocyte autophagy in heart disease: Friend or foe? (Autophagy)', *Autophagy*, 3(6), pp. 632–634. doi: 10.4161/auto.4913.

Rousseau, E. and Meissner, G. (1989) 'Single cardiac sarcoplasmic reticulum Ca2+-release channel: activation by caffeine', *American Journal of Physiology-Heart and Circulatory Physiology*, 256(2), pp. H328–H333. doi: 10.1152/ajpheart.1989.256.2.h328.

Rubler, S. *et al.* (1972) 'New type of cardiomyopathy associated with diabetic glomerulosclerosis', *The American Journal of Cardiology*, 30(6), pp. 595–602. doi: 10.1016/0002-9149(72)90595-4.

Schultz, M. B. and Sinclair, D. A. (2016) 'Why NAD+ Declines during Aging: It's Destroyed', *Cell Metabolism*. Elsevier Inc., 23(6), pp. 965–966. doi: 10.1016/j.cmet.2016.05.022.

Sciarretta, S. *et al.* (2018) 'The Role of Autophagy in the Heart', *Annual Review of Physiology*, 80(1), pp. 1–26. doi: 10.1146/annurev-physiol-021317-121427.

Scriven, D. R. L. *et al.* (2010) 'Analysis of Cav1.2 and ryanodine receptor clusters in rat ventricular myocytes', *Biophysical Journal*. Biophysical Society, 99(12), pp. 3923–3929. doi: 10.1016/j.bpj.2010.11.008.

Scriven, D. R. L., Asghari, P. and Moore, E. D. W. (2013) 'Microarchitecture of the dyad', *Cardiovascular Research*, 98(2), pp. 169–176. doi: 10.1093/cvr/cvt025.

Sedej, S. *et al.* (2010) 'Na+-dependent SR Ca2+ overload induces arrhythmogenic events in mouse cardiomyocytes with a human CPVT mutation', *Cardiovascular Research*, 87(1), pp. 50–59. doi: 10.1093/cvr/cvq007.

Sedej, S. *et al.* (2014) 'Subclinical abnormalities in sarcoplasmic reticulum Ca^{2+} release promote eccentric myocardial remodeling and pump failure death in response to pressure overload', *Journal of the American College of Cardiology*, 63(15), pp. 1569–1579. doi: 10.1016/j.jacc.2013.11.010.

Shaikh, S. *et al.* (2016) 'Regulation of cardiomyocyte autophagy by calcium', *American Journal of Physiology - Endocrinology And Metabolism*, p. ajpendo.00374.2015. doi: 10.1152/ajpendo.00374.2015.

Shannon, T. R., Ginsburg, K. S. and Bers, D. M. (2000) 'Potentiation of fractional sarcoplasmic reticulum calcium release by total and free intra-sarcoplasmic reticulum calcium concentration', *Biophysical Journal*, 78(1), pp. 334–343. doi: 10.1016/S0006-3495(00)76596-9.

Shirakabe, A. *et al.* (2016) 'Aging and Autophagy in the Heart', *Circulation Research*, 118(10), pp. 1563–1576. doi: 10.1161/CIRCRESAHA.116.307474.

Steckelings, U. M. and Unger, T. (2009) 'Angiotensin receptors and autophagy live and let die', *Hypertension*, 53(6), pp. 898–899. doi: 10.1161/HYPERTENSIONAHA.109.131425.

Taneike, M. *et al.* (2010) 'Inhibition of autophagy in the heart induces age-related cardiomyopathy', *Autophagy*, 6(5), pp. 600–606. doi: 10.4161/auto.6.5.11947.

Tanida, I., Ueno, T. and Kominami, E. (2008) 'LC3 and autophagy - Methods in Molecular Biology', *Methods in Molecular Biology*, 445(2), pp. 77–88. doi: 10.1007/978-1-59745-157-4-4.

Teng, A. C. T. *et al.* (2015) 'Metformin increases degradation of phospholamban via autophagy in cardiomyocytes', *Proceedings of the National Academy of Sciences*, 112(23), pp. 7165–7170. doi: 10.1073/pnas.1508815112.

Terman, A. (1995) 'The effect of age on formation and elimination of autophagic vacuoles in mouse hepatocytes', *Gerontology*, 41(2), pp. 319–326. doi: 10.1159/000213753.

Troncoso, R. *et al.* (2012) 'Energy-preserving effects of IGF-1 antagonize starvation-induced cardiac autophagy', *Cardiovascular Research*, 93(2), pp. 320–329. doi: 10.1093/cvr/cvr321.

Valentim, L. *et al.* (2006) 'Urocortin inhibits Beclin1-mediated autophagic cell death in cardiac myocytes exposed to ischaemia/reperfusion injury', *Journal of Molecular and Cellular Cardiology*, 40(6), pp. 846–852. doi: 10.1016/j.yjmcc.2006.03.428.

Wei, S. *et al.* (2010) 'T-tubule remodeling during transition from hypertrophy to heart failure.', *Circulation research*, 107(4), pp. 520–31. doi: 10.1161/CIRCRESAHA.109.212324.

Wettschureck, N. *et al.* (2001) 'Absence of pressure overload induced myocardial hypertrophy after conditional inactivation of Gαq/Gα11 in cardiomyocytes', *Nature Medicine*, 7(11), pp. 1236–1240. doi: 10.1038/nm1101-1236.

Woodall, B. P. and Gustafsson, B. (2018) 'Autophagy—A key pathway for cardiac health and longevity', *Acta Physiologica*, 223(4), pp. 1–11. doi: 10.1111/apha.13074.

Xiwei Zheng, Cong Bi, Marissa Brooks, and D. S. H. (1998) 'A Calcineurin-Dependent Transcriptional Pathway for Cardiac Hypertrophy', *Anal Chem.*, 25(4), pp. 368–379. doi: 10.1016/j.cogdev.2010.08.003.Personal.

Yin, Z., Pascual, C. and Klionsky, D. (2016) 'Autophagy: machinery and regulation', *Microbial Cell*, 3(12), pp. 588–596. doi: 10.15698/mic2016.12.546.

Zhang, T. *et al.* (2003) 'The δc isoform of CaMKII is activated in cardiac hypertrophy and induces dilated cardiomyopathy and heart failure', *Circulation Research*, 92(8), pp. 912–919. doi: 10.1161/01.RES.0000069686.31472.C5.

Zhang, Y. *et al.* (2011) 'Receptor-independent protein kinase Cα (PKCα) signaling by calpain-generated free catalytic domains induces HDAC5 nuclear export and regulates cardiac transcription', *Journal of Biological Chemistry*, 286(30), pp. 26943–26951. doi: 10.1074/jbc.M111.234757.

Zhu, H. *et al.* (2007) 'Cardiac autophagy is a maladaptive response to hemodynamic stress', *Journal of Clinical Investigation*, 117(7), pp. 1782–1793. doi: 10.1172/JCI27523.

Zou, Y. *et al.* (2011) 'Ryanodine receptor type 2 is required for the development of pressure overload-induced cardiac hypertrophy', *Hypertension*, 58(6), pp. 1099–1110. doi: 10.1161/HYPERTENSIONAHA.111.173500.

6 Appendix

6.1 Solutions

Table 1: Perfusion buffer

Reagent	*Cat. Nr.*	*M.W. (g/mol)*	*Amount per liter solution (g)*	*Final concentration (mmol/l)*
Sodium chloride (NaCl)	S9625	58.44	7.884	135
Potassium chloride (KCl)	P4504	74.55	0.351	4.7
Potassium phosphate monobasic (KH_2PO_4)	P5379	136.09	0.082	0.6
Sodium phosphate dibasic heptahydrate ($Na_2HPO_4 \bullet 7H_2O$)	S9390	268.07	0.161	0.6
Magnesium sulfate heptahydrate ($MgSO_4 \bullet 7H_2O$)	M 9397	246.5	0.296	1.2
HEPES ($C_8H_{18}N_2O_4S$)	H4034	238.30	2.383	10
Taurine ($NH_2CH_2CH_2SO_3H$)	T0625	125.15	3.753	30
2,3-Butanedionmonoxime ($CH_3C(=NOH)COCH_3$)	B0753	101.10	1.012	10
Glucose ($C_6H_{12}O_6$)	G7528	180.16	1.802	10

Table 2: Cannulation solution

Solution	*Cat. Nr.*	*M.W. (g/mol)*	*Quantity (ml)*	*Final concentration (mmol/l)*
Perfusion buffer, pH 7.4 at room temperature (titrated with NaOH) (see Table 2)	-	-	50	-
Calcium chloride ($CaCl_2$), 1 mol/l stock solution	21115	110.98	0.05	1

Table 3: Myocyte digestion solution

Solution or compound	*Company*	*Cat. Nr.*	*Stock Conc.*	*Volume (ml)*	*Final concentration*
Perfusion buffer, pH 7.4 at room temperature (titrated with NaOH) (for details see Table 2)	-	-	-	25	-
Liberase™	Roche	-	50 mg/10 ml	0.300	0.075 mg/ml
Trypsin 10x liquid	GIBCO	15090046	10x	0.111	0.056 mg/ml
$CaCl_2$, 1 mol/l stock solution	Sigma-Aldrich	21115	10 mmol/l	0.030	12.5 µmol/l

Table 4: Myocyte stopping solution 1

Compound	*Cat. Nr.*	*Stock Conc.*	*Volume (µl)*	*Final concentration*
Perfusion buffer, pH 7.4 at room temperature (titrated with NaOH) (for details see Table 2)	-	-	2250	-
Bovine calf serum	B8056	100%	250	10%
$CaCl_2$, 1 mol/l stock solution	21115	10 mmol/l	3.125	12.5 µmol/

Table 5: Myocyte stopping solution 2

Compound	*Cat. Nr.*	*Stock Conc.*	*Volume (ml)*	*Final concentration*
Perfusion buffer, pH 7.4 at room temperature (titrated with NaOH) (Table 2)		-	19.00	-
Bovine calf serum	B8056	100%	1.00	5%
$CaCl_2$, 1 mol/l stock solution	21115	10 mmol/l	0.025	12.5 µmol/l

Table 6: Ca^{2+} series (3 solutions containing increasing Ca^{2+} concentrations, namely 125, 250 and 500 µmol/l)

Compound	*Protocol No. or Cat. Nr.*	*Stock Conc.*	*Volume (ml)*	*Final concentration (µmol/l)*
Myocyte stopping solution 2	-	-	(1) 8.00 (2) 4.00 (3) 8.00	-
$CaCl_2$, 1 mol/l stock solution	21115	100 mmol/l	(1) 0.01 (2) 0.01 (3) 0.04	125 250 500

Table 7: Normal Tyrode solution

Compound	*Cat. Nr.*	*M.W. (g/mol)*	*Quantity (g) or volume per liter solution*	*Final concentration (mmol/l)*
Sodium chloride (NaCl)	S9625	58.44	7.948	136
Potassium chloride (KCl)	P4504	74.55	0.373	5
Magnesium chloride hexahydrate ($MgCl_2$*$6H_2O$)	M9272	203.30	0.203	1
HEPES ($C_8H_{18}N_2O_4S$)	H4034	238.30	2.383	10
Glucose ($C_6H_{12}O_6$)	G7528	180.16	1.802	10
Calcium chloride ($CaCl_2$), 1 mol/l stock solution	21115	110.98	1 ml	1

6.2 Ca^{2+} transient analysis (Matlab® based script)

```
%% read data from Excel file
clear all, close all, clc

filename_input = 'example_file.xlsx';
sheet_input = 1;

num = xlsread(filename_input,sheet_input);
time = num(:,1); period = time(2);
sig1 = num(:,2);
sig2 = num(:,3);
%sig2 = num(:,4);

index = (0:1:length(time)-1);
figure(1)
subplot(2,1,1), plot(index,sig1,'b'), xlabel('Position Index'), ylabel('Signal 1')
subplot(2,1,2), plot(index,sig2,'r'), xlabel('Position Index'), ylabel('Signal 2')

%% isolation
nt = x; % number of transients
index0 = y; % first point first transient
index1 = z; % last point first transient

n0 = index0+1; n1 = index1+1; amp = n1-n0;
sig1mat = zeros(amp+1,nt); sig2mat = zeros(amp+1,nt);
for n = 0:nt-1;
   sig1mat(:,n+1) = sig1(n0+n*amp:n0+(n+1)*amp);
   figure(2), subplot(2,1,1), hold on, plot(sig1(n0+n*amp:n0+(n+1)*amp),'b');
   sig2mat(:,n+1) = sig2(n0+n*amp:n0+(n+1)*amp);
   figure(2), subplot(2,1,2), hold on, plot(sig2(n0+n*amp:n0+(n+1)*amp),'r');
end
subplot(2,1,1), xlabel('Position Index'), ylabel('Signal 1')
subplot(2,1,2), xlabel('Position Index'), ylabel('Signal 2')

%% mean and filter
sig1mean = mean(sig1mat,2);
sig2mean = mean(sig2mat,2);
time_mean = (0:1:amp)*period;

figure(3), hold on
plot(time_mean,sig1mean,':b',time_mean,sig2mean,':r')
xlabel('Time (ms)'), ylabel('Signal')

% http://www.mathworks.com/help/signal/ref/sgolayfilt.html
sig1mean_f = sig1mean;
sig2mean_f = sig2mean;

figure(3), hold on
plot(time_mean,sig1mean_f,'b',time_mean,sig2mean_f,'r')

%% analysis
signal = sig1mean_f;
   sig_min = min(signal);
   [sig_max ind_max] = max(signal);
   sig_amp = sig_max-sig_min;
   sig_ttp = time_mean(ind_max);
   frac = 0.5;
   vec_rt = find(signal(ind_max:end)<sig_max-frac*sig_amp); ind_rt = vec_rt(1);
   sig_rt50 = time_mean(ind_max+ind_rt-1)-time_mean(ind_max);
   frac = 0.9;
   vec_rt=  find(signal(ind_max:end)<sig_max-frac*sig_amp); ind_rt = vec_rt(1);
```

```
   sig_rt90 = time_mean(ind_max+ind_rt-1)-time_mean(ind_max);
sig1_min = sig_min
sig1_max = sig_max
sig1_amp = sig_amp
sig1_ttp = sig_ttp
sig1_rt50 = sig_rt50
sig1_rt90 = sig_rt90

signal = sig2mean_f;
   sig_min = min(signal);
   [sig_max ind_max] = max(signal);
   sig_amp = sig_max-sig_min;
   sig_ttp = time_mean(ind_max);
   frac = 0.5;
   vec_rt = find(signal(ind_max:end)<sig_max-frac*sig_amp); ind_rt = vec_rt(1);
   sig_rt50 = time_mean(ind_max+ind_rt-1)-time_mean(ind_max);
   frac = 0.9;
   vec_rt = find(signal(ind_max:end)<sig_max-frac*sig_amp); ind_rt = vec_rt(1);
   sig_rt90 = time_mean(ind_max+ind_rt-1)-time_mean(ind_max);
sig2_min = sig_min
sig2_max = sig_max
sig2_amp = sig_amp
sig2_ttp = sig_ttp
sig2_rt50 = sig_rt50
sig2_rt90 = sig_rt90

%% Write results into a new Excel file
% filename_output = strcat(filename_input,'_results2.xlsx');

filename_output = '1_results.xlsx';

%%------------ filename -----------------
filename_output = strcat('results_',filename_input);
if ~strcmp(filename_output(end),'x')
   filename_output=strcat(filename_output,'x');
end
%%---------- filename ---------------
sheet_output = 1;

output = {'Time','Signal 1','Signal 2'};
xlswrite(filename_output,output,sheet_output,'A1')

output = [time_mean' sig1mean_f sig2mean_f];
xlswrite(filename_output,output,sheet_output,'A2')

output = {'Measure','Signal 1','Signal 2';...
   'min', sig1_min, sig2_min;...
   'max', sig1_max, sig2_max;...
   'amp', sig1_amp, sig2_amp;...
   'ttp', sig1_ttp, sig2_ttp;...
   'rt50',sig1_rt50,sig2_rt50;...
   'rt90',sig1_rt90,sig2_rt90;};
xlswrite(filename_output,output,sheet_output,'E1')
```